ATTACHMENT 9

REACTIVITY FROM NEUTRON POWER SPECTRAL DENSITY MEASUREMENTS WITH CF-252

JOHN T. MIHALCZO
W. T. KING
OAK RIDGE NATIONAL LABORATORY

PRESENTED TO NUCLEAR REGULATORY COMMISSION
SEPTEMBER 22, 1980

8011070128

PRINCIPLE OF MEASUREMENT

Cf-252 NEUTRON SOURCE DRIVEN NEUTRON NOISE ANALYSIS

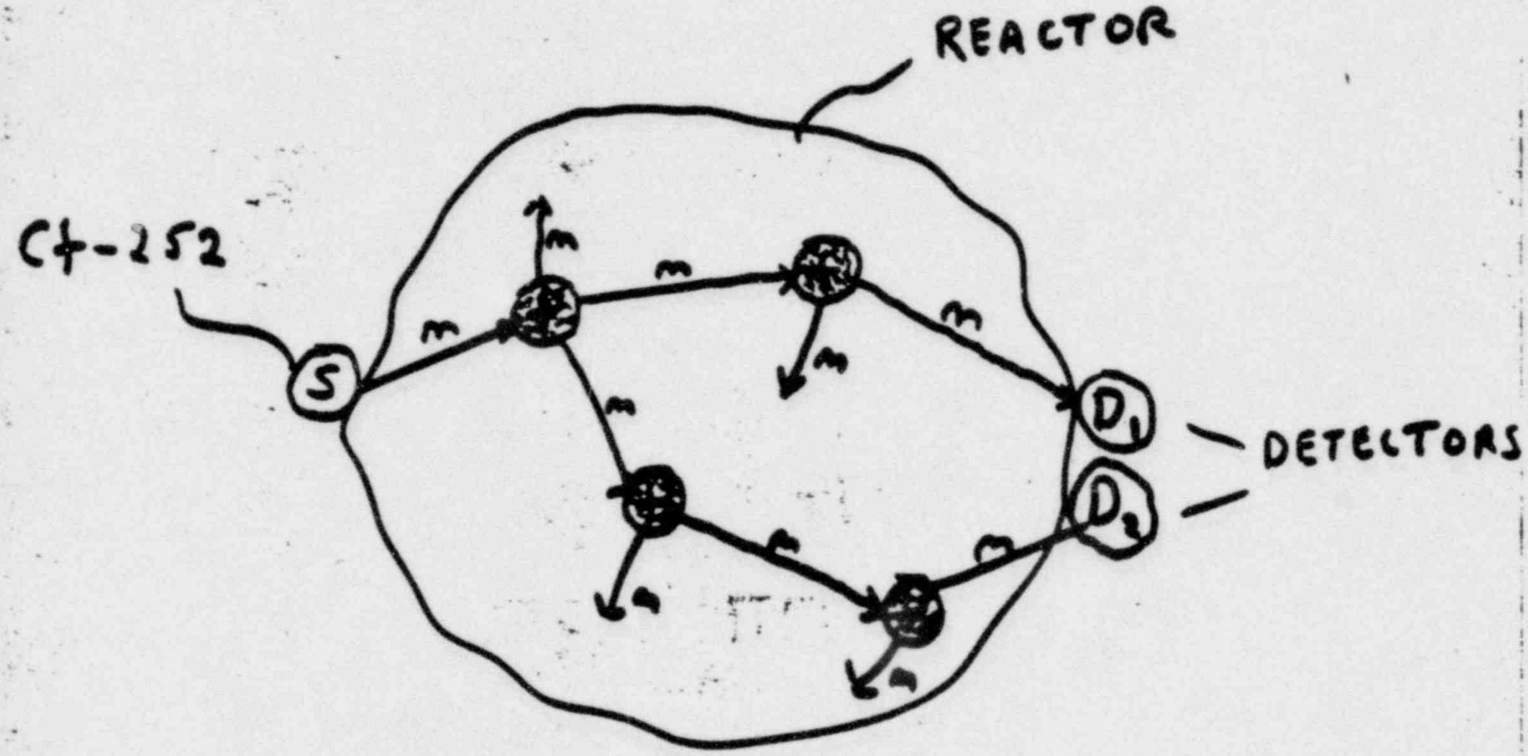

RELATIONSHIP BETWEEN SPECTRAL DENSITY AND NEUTRON MULTIPLICATION FACTOR

$$\frac{\Delta K}{K} = C \, \frac{G^{*}_{S1} \, G_{S2}}{G_{11} \, G_{23}}$$

K = MULTIPLICATION FACTOR

C = CONSTANT

ADVANTAGES OF THIS METHOD

1. OBTAINS REACTIVITY FROM MEASUREMENTS ON ONLY THE SUBCRITICAL STATE OF INTEREST THUS IT DOES NOT NEED A REFERENCE MEASUREMENT NEAR CRITICAL.

2. INTERPRETATION DOES NOT DEPEND ON RELATIVE OR ABSOLUTE VALUES OF THE REACTOR INHERENT SOURCE OR OF DETECTION EFFICIENCY.

FY-80 ACCOMPLISHMENTS

- STATIC 2-DIMENSIONAL DIFFUSION THEORY CALCULATIONS WERE PERFORMED WITH 3-GROUP CROSS SECTIONS FROM G.E. FOR THE ZIMMER CORE USING VENTURE

- FX2TH, A 2-DIMENSIONAL TIME DEPENDENT DIFFUSION THEORY CODE WAS OBTAINED FROM ANL AND HAS RUN THE STANDARD TEST CASE (9 GROUP 25 X 40 MESH LMFBR ROD DROP PROBLEM)

STATIC DIFFUSION THEORY RESULTS

- MULTIPLICATION FACTORS FROM VENTURE AGREE WITH THOSE CALCULATED AT G.E.
- CENTRAL DETECTION EFFICIENCY FOR ZIMMER AT INITIAL START UP WITH ALL RODS INSERTED BUT THE CENTRAL IS $\sim 10^{-4}$ COUNTS/FISSION FOR A 5 GM FISSION CHAMBER
- DETECTION EFFICIENCY FOR LI GLASS SCINTILLATORS WHICH COULD BE USED IN INITIAL LOADING WOULD BE AT LEAST A FACTOR OF 10 HIGHER ALLOWING MEASUREMENTS IN LESS THAN 1 HOUR

BASIC APPROACH TO THE EVALUATION OF SPATIAL EFFECTS

- CALCULATION OF IMPULSE RESPONSE AND FROM IT MEASURED SPECTRAL DENSITIES USING
  - NODAL KINETICS
  - 2D TIME DEPENDENT DIFFUSION THEORY
  - 2D JPRKINETICS
- MONTE CARLO METHODS

USING OTHER FUNDING, SPECTRAL DENSITY MEASUREMENTS WITH 252-Cf FOR A 5% ENRICHED URANYL FLUORIDE SOLUTION WERE RECENTLY COMPLETED

- GEOMETRY - 22" DIAMETER CYLINDER

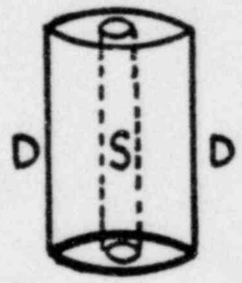

- MEASUREMENTS WERE SUCCESSFULLY COMPLETED BETWEEN A DELAYED CRITICAL HEIGHT 14.4 IN. AND 8" (~ 1/2 CRITICAL HEIGHT)

- OUR CURRENT PROGRAM CALLS FOR US TO PREDICT THE EXPERIMENT RESULTS FOR A FULLY LOADED BWR.

- IN ADDITION - WE PROPOSE TO BENCHMARK OUR CALCULATION METHODS BY CALCULATING THE RESULTS OF THE RECENT SOLUTION EXPERIMENT.

ATTACHMENT 10

EXPERIENCE AT HITACHI ENERGY RESEARCH LABORATORY

1/80 - 5/80

Report to NRC Review Group on Noise Surveillance and Diagnostics 9/22/80

Requested by Mr. W. S. Farmer

by: Robert W. Albrecht
Professor
Dept. of Nuclear Engineering
University of Washington
Seattle, Washington 98195

Summary

Experience in the area of noise surveillance and diagnostics at Hitachi Energy Research Laboratory gained during the period 1/80 to 5/80 as a consultant to the laboratory is discussed in this report. The Energy Research Laboratory, Hitachi, Ltd. is a diverse industrial laboratory whose mission is to support the activities of Hitachi, Ltd. in energy development. To put this report in perspective, a brief review of the organization and general activities of the Hitachi Energy Research Laboratory preceeds discussion of activities in the area of noise surveillance and diagnostics.

Specifically, the experience in noise surveillance and diagnostics discussed in this report relates to three general subjects:

(1) loose parts monitoring

(2) operator/computer interaction for abnormal condition control

(3) BWR transient and stability calculations

HITACHI ENERGY RESEARCH LABORATORY ORGANIZATION

General Manager
K. Taniguchi

Assoc. General Manager
S. Yamada

1st Department	2nd Department	3rd Department	Planning Dept.
Mgr., S. Kobayashi	Mgr., Y. Kato	Mgr., A. Doi	Mgr., Ueda
58 persons	50 persons	60 persons	? persons

1st Department — Units/Leaders

1. BWR core design (Takeda)
2. Core Mgmt. & Automation (Motoda)
3. Control & Algorithm Development (Kikuchi)
4. FBR cores & Fusion Design (Inoue)
5. Reliability & Safety (Osawa)
6. Control & Instrumentation (Watanabe)

2nd Department — Units/Leaders

1. Core heat transfer (Yamanouchi)
2. Fusion Expts. & Instr's. (Nishi)
3. In-service Inspection (Suzuki)
4. FBR materials (Shimoyashiki)
5. BWR Instr's & Cont. eqpt. (Ito)
6. FBR Heat Transfer (Suzuoki)
7. BWR Safety (Sumita)
8. Flow Induced vibe (Kotani)
9. New Energy (Sumita)

3rd Department — Units/Leaders

1. Uranium Enrichment
2. Uranium Enrichment
3. Rad Waste treatment
4. Mat'l Science & water chemistry
5. Remote Control & automation
6. Rad waste chemistry
7. Diagnostics (Izumi)
8. Health Physics

1. Loose Parts Monitoring

HERL research personnel:
S. Izumi
Y. Michiguchi
K. Yamada
Y. Ichikawa

Activities: Triangulation of BWR accelerometer data for impact location and pattern recognition for amplitude - time delay accelerometer data.

Conclusions: (1) Triangulation of accelerometer responses is capable of locating the position at which sonic energy of an impact within or on a BWR vessel arrives at the vessel surface. The resolution achieved for an actual BWR vessel is to locate the impact to a zone having an area of $10m^2$ or about 3.3% of the vessel area with high probability. This result could be improved upon with a more optimum array of sensors.

Success in triangulation is subject to three conditions:

(a) Adequate signal to noise ratio
(b) Favorable geometric arrangement of sensors
(c) Simple sonic connection from impact point to vessel

If these three conditions were not met, the triangulation method failed.

(2) Attempts to use both relative amplitude and time delay of accelerometer signals to produce a two dimensional pattern for impact location have proven unsuccessful due to the fact that a distinct initial amplitude is not exhibited by accelerometer signals for impacts far from the sensor.

Background

An extensive set of tests was performed using five special accelerometers installed on the Shimane BWR.* The experiments were performed by personnel from Hitachi Energy Research Laboratory and several utilities. The reactor had the vessel head and upper components such as steam driers removed. Various structures inside and outside the vessel were impacted with a calibrated hammer and the relative time of arrival of the acoustic energy at each transducer was recorded.

Experimental configuration and expectations

The sensors were arranged at the locations listed in Table 1.

Sensor No.	Component	Elevation (Meters)	Azimuth (°)	Distance from Vessel Surface
1	Feedwater pipe	11.7	135	1.2
2	RCS piping	11.3	90	2.2
3	PLR inlet piping	7.2	300	1.2
4	PLR outlet piping	3.2	180	1.5
5	Lower vessel wall	1.5	190	0.0

Figure 1 shows a cylindrical reactor vessel with the cylinder "unwrapped" and extended. This type of figure will be generally used in discussing the results of this analysis. The locations of the five sensors on the reactor vessel are given on Figure 1. Notice that the pair of sensors (1.2) and also the pair (4,5) are located close together so that, from the point of view of triangulation, there are three effective zones of detectors on the vessel. The circles on Figure 1 are drawn with radii of 0.7 meters since the experiments exhibited an uncertainty in arrival time of signals of about $\pm$ 0.2 msec and the average sonic speed on the vessel was about 3.3 meters/msec resulting in an uncertainty of about 0.7 meters.

A typical disturbance location, labeled "A" is also shown in Figure 1. Location "A" is equidistant from sensors 2,3,4. The cross-hatched zone around disturbance "A" represents the uncertainty in the location of "A" by measurements from sensors 2,3,4 if the only undertainty is the time delay variation. Since sensors 1 and 5 are close to 2 and 4, respectively, their added information does not decrease the uncertainty in the location of "A" very much.

Other typical disturbance locations labeled "B" and "B'" are also shown on Figure 1. Both locations are at the same relative distance to sensors 3 and 4 with the distance to 3 about 1.3 meters shorter than the distance to 4. However, if the disturbance is at B, its shortest path to 3 is down the cylinder turning through positive angles but from B' the

*Actually, seven sensors were installed, but two of them were below the bottom of the vessel on a CRD housing and an LPRM housing and were not useful for triangulation.

shortest distance to 3 is to propagate turning negatively through the azimuth. The cross-hatched areas show the uncertainty in B and B' as measured in both directions and being consistent with a similar response time from sensor 2. It is seen that the uncertainties overlpa. This means that there is an ambiguity in addition to an uncertainty in the location of an impact in the region of B or B' caused by the non-optimum placement of sensors with respect to locating a disturbance in this region. Also, the responses of sensor 1 and 5 will not help to resolve this ambiguity since a wave from B or B' is well within the response uncertainties of these sensors.

Actually, there are additional uncertainties that make the triangulation result less accurate. The speed and mode of propagation of sonic waves on the vessel is not known accurately. In calibration experiments, the sound speed from one sensor to another was found to bary from about 2 to 4.6 meters/msec. From point "A" to sensors 2,3,4, (distance = 5.7 meters), this uncertainty of $\pm$ 1.3 meters/msec introduces an uncertainty in the knowledge of propagation speed. This represents an area of about 4.8 meters^2 or about 1.6% of the area of the vertical surface of the reactor vessel. Thus, the uncertainty in propagation speed may be twice as large as the uncertainty due to time delay variation for a favorably located disturbance and this uncertainty will also amplify the ambigutiy associated with locating a disturbance in a remote region.

Another uncertainty may be important. Four of the five detectors are located on pipes attached to the BWR vessel. Only sensor 5 is on the vessel. In the triangulation method explored here, all signal arrival times are referenced to thier arrival at the junction of the vessel and the pipe carrying the sensor. Typical distances from vessel to sensor are 1.2 to 1.5 meters. At 3.3 meters/msec, the average delay is about 0.4 msec for a sonic disturbance to travel from the vessel to the sensor. If the uncertinty in speed is $\pm$ 1.3 meters/msec, in 3.3. meters/msec (or about 40%), then the uncertainty in arrival time at the vessel-pipe junction may average about $\pm$ 0.16 msec. This is comparable to the standard deviation in time delay of $\mp$ 0.2 msec that was generally observed in the experiments. Therefore, this uncertainty could produce an uncertainty in locating a central (to the detector array) disturbance of about 2.5 meters^2. As before, more serious effects are expected for peripherally located disturbances.

If all of the above uncertainties were additive, then one would expect the potential error in the location of a central disturbance to be about 10 meters^2. Or, stated in terms of percentages, one would expect that the location of a disturbance on the vessel should be within an area representing about 3.3% of the total area of the vertical sides of the vessel if the disturbance is in a central location and larger uncertainties plus ambiguities of the disturbance is located far from the sensor array.

These estimated uncertainties are used in the analysis method. The most probable estimate of the impact location is found from a circular area of 10 square meters (diameter of 3.6 meters) where intersections of triangulations are most dense. This estimate is believed to be such that one can have reasonably high confidence that the impact is located within this area if the impact is not in an ambiguous region of the vessel.

A more optimistic estimation is also given by a circular area of 2.5 square meters (diameter 1.8 meters) that is derived from the minimum estimated uncertainty. The likelihood that the impact falls within this area is smaller than for the most probable estimate but the decrease in confidence is unknown.

Analysis method

The above discussion of expected uncertainties makes it clear that an extremely detailed model of the geometry of the reactor vessel and a detailed analysis of sonic propagation characteristics would not be compatible with the accuracy expected from the experimental results. In this section of this report, the basic assumptions of the methods are listed, the technique used for calibration is described, and an example of the method of triangulation is presented.

Assumptions

(1) Sonic waves due to an impact travel from the point of impact to the vessel at the closest point of connection between the structure being impacted and the vessel.
(2) Sonic waves travel from the point that they reach the vessel to the point that structures containing accelerometers are attached to the vessel by the shortest path on the vessel surface.
(3) Sonic waves travel from the vessel surface along the structures containing accelerometers to the sensors by the shortest path.
(4) The speed of propagation of a sonic wave from one sensor to another is determined by the average value of measured delay times from impacts near one transducer and responses at the other transducers.
(5) In all cases, the speed of propagation of sonic energy from an impact to a sensor is assumed to be best approximated by the average speed measured from all other sensors to the sensor in question.
(6) The speed of propagation of sonic energy along the structure carrying a sensor is assumed to be the same average speed used in (5).

Calibration

The calibration of the sensor array for carrying out the triangulation is performed as follows:

(1) Impacts are produced near each sensor and the delay time to every other sensor is determined (assumption 4) by averaging 10 trials for each sensor.
(2) The total distance of travel of sonic waves from the reference sensor to each other sensor is determined using assumptions 1,2, and 3 above.
(3) The speed of propagation to each sensor is determined using assumption 5.
(4) A time delay from the vessel surface to the sensor position is calculated from assumption 5 and the known distance of the sensor from the vessel surface (assumption 3).

For the case of the Shimane reactor with sensors placed as noted in Table 1, the results of carrying out calibration stpes 1 to 4 are summarized in Tables 2 and 3.

Table 2. Calibration Results

IMPACT SENSOR NO. \ RESPONSE SENSOR NO.		1	2	3	4	5	
1		—	5.4 2.6±0.1 2.08	10.9 3.3±0.2 3.30	11.4 2.6±0.1 4.38	11.7 3.2±0.2 3.66	total dist. (M) time delay (msec±) speed (M/msec)
2		5.4 1.4±0.2 3.86	—	11.1 2.7±0.1 4.11	12.7 2.7±0.1 4.70	12.9 3.2±0.5 4.03	" " "
3		10.9 4.1±0.2 2.66	11.1 4.9±0.3 2.27	—	9.3 2.9±0.3 3.21	8.7 2.3±0.3 3.78	" " "
4		11.4 3.3±0.4 3.45	12.7 not det'd	9.3 2.8±0.3 3.32	—	3.2 0.9±0.1 3.56	" " "
5		11.7 4.2±0.9 2.79	12.9 4.3±0.6 3.0	8.7 2.2±0.1 3.95	3.2 0.7±0.1 4.57	—	" " "
		3.19	2.45	3.67	4.21	3.76	ave. speed to each sensor (M/msec)

Table 3. Time Delays from Vessel Surface to Sensor

Sensor No.	Distance (M)	Speed (M/msec)	Time Delay (msec)
1	1.2	3.19	0.38
2	2.2	2.45	0.9
3	1.2	3.67	0.33
4	1.5	4.21	0.36
5	0.0	3.76	0.0

Triangulation procedure

(1) The relative time delays to each sensor are measured for an impact at an arbitrary location.

(2) For each sensor, the time delay listed in Table 3 is subtracted from the arrival time at the sensor to produce estimated times that sonic energy arrives at the connection between the sensor-supporting structure and the vessel.

(3) The relative order of arrivals at the sensor structure-vessel interface is inspected to determine a zone of possible points on the vessel where the impact energy reached the vessel. Uncertainties are taken into account.

(4) Time delays between arrivals at the sensor structure-vessel interface are normalized to $t = 0.0$ for the first arrival and all time delays are converted to distances using the average speeds of propagation given in Table 2.

(5) Triangulation between sensor pairs using the relative distances computed in (4) is performed to determine all loci of possible impact positions for pairs of sensors that lie in the zone of possible points determined in (3).

(6) The loci of possible impact positions are inspected for the density of intersections and the area(s) of the most likely impact position(s) is determined as a 10 meter^2 circle. If warranted, circles of 2.5 meter^2 are explored for more accurate impact location.

Example

This six step procedure can be illustrated with an example.

A set of 10 impacts was applied to the feedwater pipe, external to the vessel, and attached to the vessel at the 45° position and an elevation of 11.7 meters. The response times of the five sensors were observed to be:

(1)

Sensor No.	Time Delay (msec)
1	0.0
2	0.2 ± 0.2
3	0.8 ± 0.2
4	1.2 ± 0.3
5	1.9 ± 0.3

(2) The times of arrival of sonic energy at the sensor structure-vessel interface are determined by using the delay times from Table 3. The uncertainty for sensor #1 is taken to be 0.2 msec.

Sensor No.	Relative arrival time of sonic energy at sensor structure-vessle interface
1	0.2 ± 0.2
2	0.3 ± 0.2
3	1.2 ± 0.2
4	1.5 ± 0.3
5	2.6 ± 0.3

(3) The apparent relative order of arrival of sonic energy (normalized to 0.0 for the first arrival) at the sensor structure-vessel interface is (ignoring insignificant figures):

Sensor No.	Relative apprival time at sensor structure-vessel interface
2	0.0 $\pm$ 0.2
1	0.3 $\mp$ 0.2
3	1.2 $\mp$ 0.2
4	1.5 $\mp$ 0.3
5	2.6 $\mp$ 0.3

It can be seen that sensors 2 and 1 have overlapping uncertainties, so it is not certain which order is appropriate, 2-1 or 1-2. Obviously, it is more likely that the correct sensor order is 2-1. It is clear that sensors 3,4, and 5 definitely lag 1 and 2. there is ambiguity between the order of sensors 3 and 4 but it appears that 5 definitely lags all others, in particular, 3.

Figure 2 shows the zones of possible points of origin of the impact that are compatible with this order of arrival. The lines on the boundary of the zones are labeled to show from which sensor order they drive. The points to the "left" of the 1 > 2 dividing line (shown dashed since it is uncertain) allow arrival time orders of 2-1-3-4-5 or 2-1-4-3-5. The points to the "right" of the 1 > 2 dividing line allow arrival time orders of 1-2-3-4-5 or 1-2-4-3-5. The most probable order is 2-1-3-4-5. This zone is shown in Figure 2 in cross hatch. The second most probably zone is judged to be 2-1-4-3-5 and is shown with hatching from 135° to -45° in Figure 2. The third probable zone is assumed to be 2-1-3-4-5. This is shown in hatching from -135° to 45° in Figure 2. The least probable zone is shown surrounded by shaded zones and is left unshaded

The total area of all probable zones for the impact as determined from the order of arrival of signals is 148 meters^2, or about 48% of the vessel surface. The area of the most probable zone is 72 meters^2 or 23.5% of the vessel surface. It is seen from this analysis that the consideration of only the order with which sonic energy arrives at the sensor structure-vessel interface has eliminated over 50% of the vessel surface as a candidate for the source of the sonic energy and, with relatively high probability, the analysis has actually eliminated over 75% of the vessel surface as the origin of the impact.

(4) Triangularization is performed by simply finding the loci of all points in the allowed sensor order zone that intersect one detector and are tangent to a circle of a radius equal to the time delay to a later detector. The distance corresponding to the time delay is computed using the sonic speeds to each detector given in Table 2.

For the example problem of the impact at feedwater pipe 45°, the relative distances corresponding to the observed time delays are:

DELAYS IN METERS

FROM \ TO	1	3	4	5
2	1.0	4.4	6.3	9.8
1		3.3	5.1	8.6
3			1.3	5.3
4				4.1
	....	- - - - -	—·—·—	═══

On Figure 3, all loci in zone 2-1-3-4-5 are shown with the types of lines noted at the lower row of the above table. The uncertainties in data have not been explicitely used in this step. The loci in other zones have many fewer intersections and are not shown. A total of 40 intersections of loci are found in zone 2-1-3-4-5. However, these intersections are concentrated in a region in the vicinity of 45° - 100° of azimuth and 8 to 13 meters in vessel elevation.

Figure 4 shows estimates of the impact position from this data. The large circle has sn area of 10 meters^2 and encompasses the most number of intersections that can be surrounded by such a circle. In this case, 32 of the 40 intersections in zone 2-1-3-4-5 lie in the circle having an area of 10 meters^2. That is, an area of 14% of the most probable zone as determined by order of signal arrival contains 80% of the estimates made by triangulation. Therefore, the most probable estimate of the impact location is judged to be in this area centered at 59° and 11 meters with an uncertainty of 10 meters^2 or 3.3% of the vessel area.

Three smaller circles of an area of 2.5 meters^2 are also shown in Figure 4. Each of these circles encloses 12 intersections. Therefore, these more refined estimates of the impact location must be considered equally probable. These estimates are centered at

2.5 m^2 estimate designation	Azimuth	Elevation
A	59°	11.7 m
B	5[illegible]°	10.5 m
C	8[illegible]°	10.3 m

The actual impact occurred on the feedwater pipe at 45° with an elevation of 11.7 meters. Estimate "A" encloses this location as does the most probable estimate with 10 m^2 uncertainty.

This example shows a case where the following conclusions can be drawn:

(a) The position at which the sonic energy of the impact reached the reactor vessel has been localized to 10 m^2 (3.3% of the reactor vessel area) with no apparent ambiguity.

(b) The position at which the sonic energy of the impact reached the reactor vessel has been estimated to be at one of three locations of area 2.5 m^2 (0.8% of reactor vessel area) with equal probability.

(c) One of the smaller areas (A) encloses the actual position where good judgement ascertains that the sonic energy from the impact reached the reactor vessel. The distances from the center of the estimates to the actual impact location in the three cases are 0.5, 1.4, 2.2 meters for A, B, C respectively.

Results

A procedure identical to that just described was carried out for eight different test impacts including the one just described. The remaining seven tests were for impacts inside the Shimane reactor vessel with the head and much of the upper structure removed. The results are tabulated according to the following shceme:

IMPACT	The actual position of the test impact (5 trials)
ORDER AREA	The total area of estimation allowed by the sensor order criterion (in m^2 and %)
ORDER AREA (1)	Area of most probable order zone (in m^2 and %)
MP ESTIMATE	Position of most probable 10 m^2 = 3.3% estimate of location at which sonic energy reached reactor vessel
MP(2) ESTIMATE	Secondary estimate of 10 m^2 area of impact
ESTIMATE (i)	The location of the i'th local estimate (2.5 m^2) of impact location with i = 1,2,... increasing with decreasing numbers of intersections in the local estimate area
IMPACT LOCATION	An estimate from structural considerations of the position at which the impact energy reaches the reactor vessel

The example just presented in detail is tabulated in Table 4 as case #1. The (1.2.3) preceding each local estimate for case #1 implies that each local estimate is equally probable (has same number of intersections). Only case #3 also shows an equal likelihood of local estimates.

Table 4 summarizes the results obtained in the eight tests presented in this paper.

Table 4. Summary of results

CASE #	IMPACT	ORDER AREA (m^2 & %)	ORDER AREA(1) (m^2 & %)	HP ESTIMATE (^{o} & elev.)	HP(2) ESTIMATE (^{o} & elev.)	LOCAL ESTIMATE (i) (^{o} & elev.)	IMPACT LOCATION (^{o} & elev.)
1	Feedwater pipe 45^o	$148m^2$ 48%	$72m^2$ 23.5%	59^o 11m	——	(1,2,3) 59^o 11.7m (1,2,3) 57^o 10.5m (1,2,3) 83^o 10.3m	45^o 11.7m
2	Feedwater Sparger 90^o	$12.5m^2$ 4%	$12.5m^2$ 4%	144^o 9.4m	——	(1) 121^o 10m (2) 155^o 8.9m	100^o 11.7m
3	Feedwater Sparger 135^o	$12.5m^2$ 4%	$12.5m^2$ 4%	137^o 9.8m	——	(1,2) 110^o 10.6m (1,2) 117^o 9.7m	135^o 11.7m
4	RCS Sparger 90^o	$143.7m^2$ 47%	$12.5m^2$ 4%	135^o 9.7m	——	(1) 122^o 10.4m (2) 126^o 9m	90^o 11.3m
5	Drier Bracket 45^o	$148m^2$ 48%	$72m^2$ 23.5%	81^o 10.7m	41^o 16.5m	(1) 89^o 10.1m	45^o 16.5m
6	Drier Bracket 315^o *	$191m^2$ 62%	$63m^2$ ** 20.5%	171^o 10.6m	236^o 17.6m	(1) 180^o 9.9m (2) 243^o 18.4m	315^o 16.5m
7	Shroud Bracket 0^o	$25.8m^2$ 8.4%	***	270^o 12.6m	11^o 6.8m	—	****
8	Shroud Bracket 180^o	*****					****

* Impact energy for drier bracket 315^o only 1/3 of impact energy of all other cases

** The most probable zone does not include the impact location

*** The most probable zone is undefined because no area on the vessel corresponds to the impact order

**** The sonic connection from the shroud bracket (which is not directly attached to vessel) is complicated

***** The order of arrivals cannot be satisfied by any position on the vessel

Discussion of results

The results obtained from these attempts to locate an impact by triangulating accelerometer response times on a BWR vessel illustrate that several conditions are necessary (and, perhaps, sufficient) for a simple triangulation to yield reasonable results.

The first condition is that the signal to noise ratio of the basic sonic propagation energy is sufficiently large to produce clear impulsive signals at the transducers. Since these tests were performed with the reactor shut down and partially disassembled, there was very little interfering noise from pump and flow induced vibration and this condition did not meet a severe test in this set of experiments. However, case #6 may provide some information on the effect of reducing signal level. In comparison to case #5 it is seen that the two cases are both for impacts applied to a drier bracket and in both cases the sonic connection to the vessel is direct. In case #5 the impact energy was 0.6 joules and a marginal estimate (MP(2)) of the impact zone was achieved. In case #6 the impact energy was 0.2 joules and the result was such that no really satisfactory estimate of the impact zone was produced. This difference between case #5 and case #6 may be partially explained by the difference in impact energy although caution should be used in light of the fact that the relationship between the detector array and the impact is different in the two cases. No investigation of signal to noise ratio requirements was performed as part of this study but the conclusion that a sufficient signal to noise ratio is required for triangulation is abundantly clear. This condition may be difficult to meet in an operating reactor.

A second condition is that the geometric arrangement of the transducers is suitable for triangulation. Cases #1 to #4 all were for impacts that occurred at levels in or on the vessel that were similar to the position of the top-most sensor. Cases #1 and #3 produced most probable estimates in good agreement with the impact location and cases #2 and #4 produced a marginal, most probable estimate. The errors of about 45° in azimuth in these latter cases represent distances of two meters. On the other hand, cases #5 and #8 were for impacts at a location considerably above the highest transducer on the vessel. Uncertainties and ambiguities can be expected in these cases. The most probable estimate is never in agreement with the impact location. However, in case #5 the second most probable estimate is in good agreement with the impact location. This contrast between the results achieved as a function of location illustrates the necessity that the geometric arrangement of detectors be suitable for triangulation.

The method used for impact location makes the assumption that the impact energy is transmitted from the point of impact to the vessel at a unique point. For this to be true, there must be a relatively simple connection between the structure being impacted and the vessel without multiple sonic propagation paths that would complicate the location of the point at which sonic energy reaches the vessel. This condition was reasonably well satisfied for cases #1 to #6. Cases #1 to #5 all produced reasonable estimates of the impact location and case #6 failed although a lower impact energy was employed and this may have contributed to the failure. In cases #7 and #8 the shroud bracket is not directly connected to the vessel and the sonic path from the impact to the vessel is complicated. The results of cases #7 and #8 are judged to be uninterpretable in terms of the simple theoretical framework used for this analysis. To interpret such cases, it will be necessary to employ a much more sophisticated analysis method that takes multiple sonic paths into account.

The importance of good temporal resolution and a favorable geometric arrangement of detectors is illustrated by cases #2 and #3. In these cases, the order of reception of signals alone served to define the impact location to an area of 12.5 m^2. The reason for these results is that the time resolution and geometric location of detectors was such that the order of signal reception narrowed the search area to a triangular region in both cases. Figure 5 illustrates the triangular area defined by the order relationships that the response of detector 4 follows sensors 1 and 2 in addition to the relationship that the response of sensor 3 lags sensor 4.

These examples show that if sensor placement is chosen judiciously to define a restricted zone for the impact location and if the time resolution is good enough to determine the order of sensor response with great certainty, then the region of the impact can be isolated to a reasonably small zone (in this example, 12.5 m^2 = 4 of vessel area) without using the specific relative time delay information at all. However, use of the time delay information by simple triangulation may serve to refine the estimate of impact location provided by the order in which sensors respond.

FIGURE 1. LOCATION OF SENSORS ON SHIMANE BWR, UNCERTAINTY IN ARRIVAL TIME AT SENSORS, TYPICAL UNCERTAINTIES AND AMBIGUITIES EXPECTED IN IMPACT LOCATION.

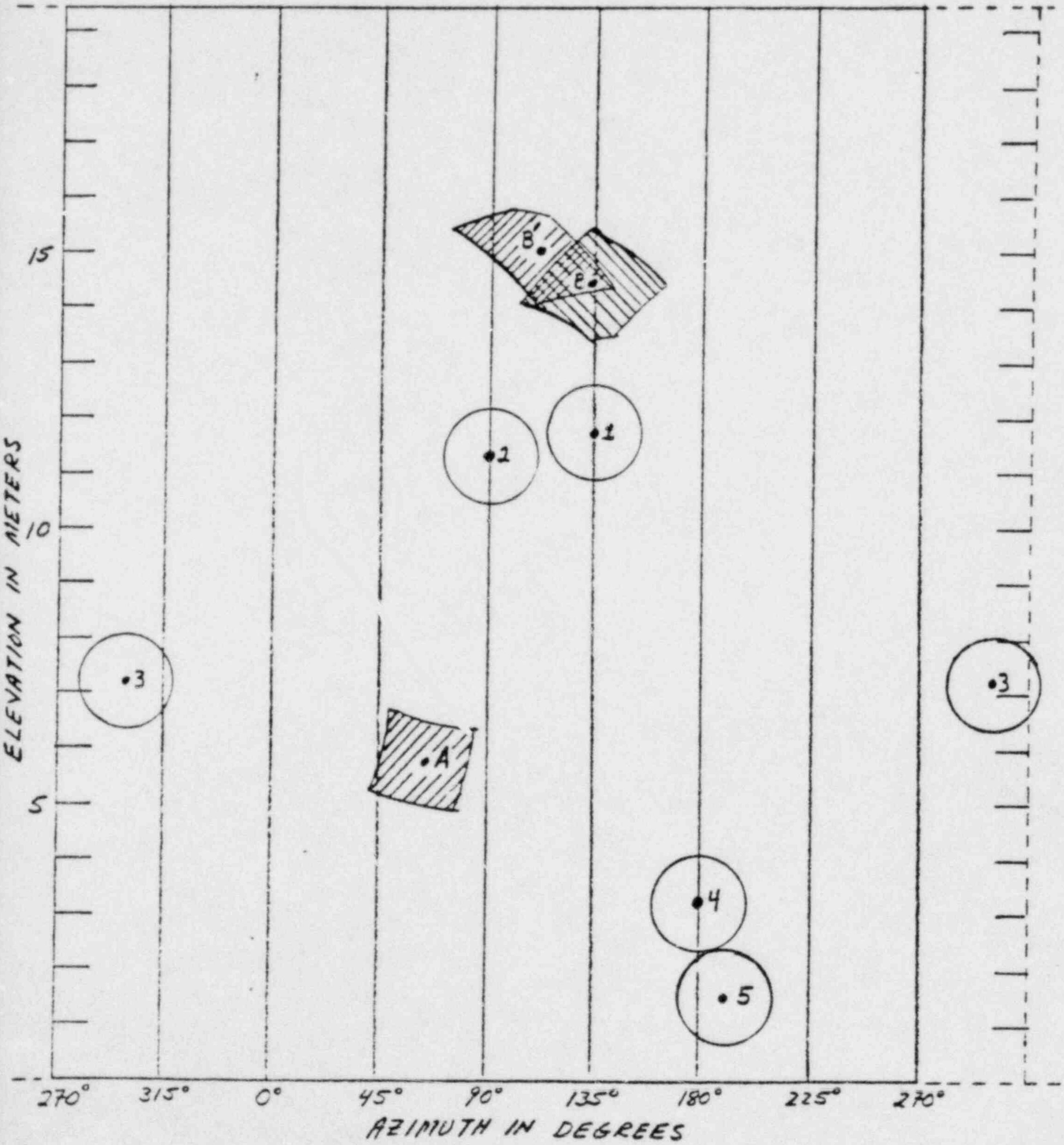

FIGURE 2. ZONES OF IMPACT ORIGIN ACCORDING TO ARRIVAL ORDER FOR CASE #1, FEEDWATER PIPE - 45°

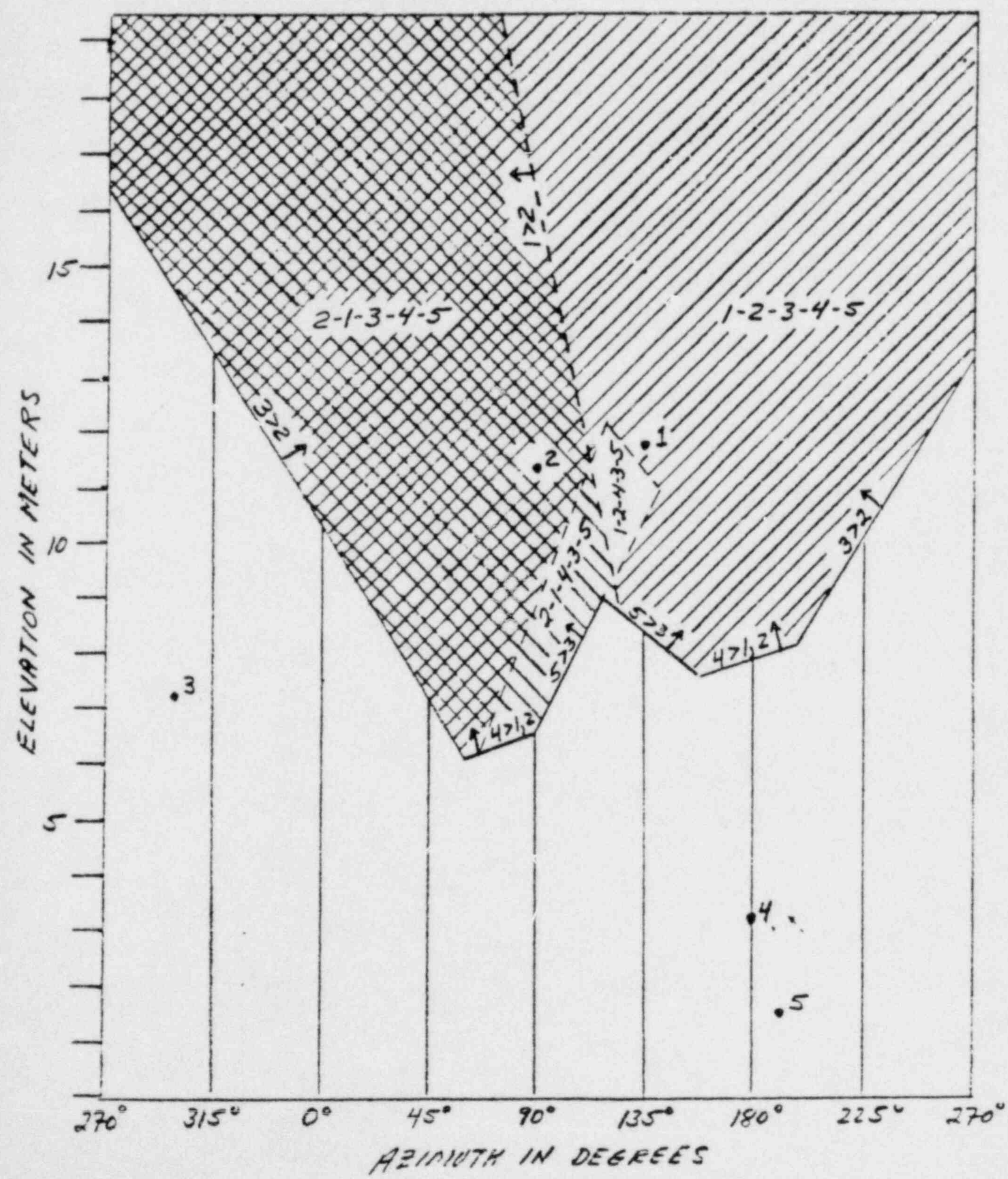

FIGURE 3. LOCI OF TRIANGULATION PAIRS IN ORDER ZONE 2-1-3-4-5 FOR CASE #1, FEEDWATER PIPE -45°

REFERENCE DETECTOR	LOCUS TYPE
1	....
3	- - - - -
4	—·—·—
5	————

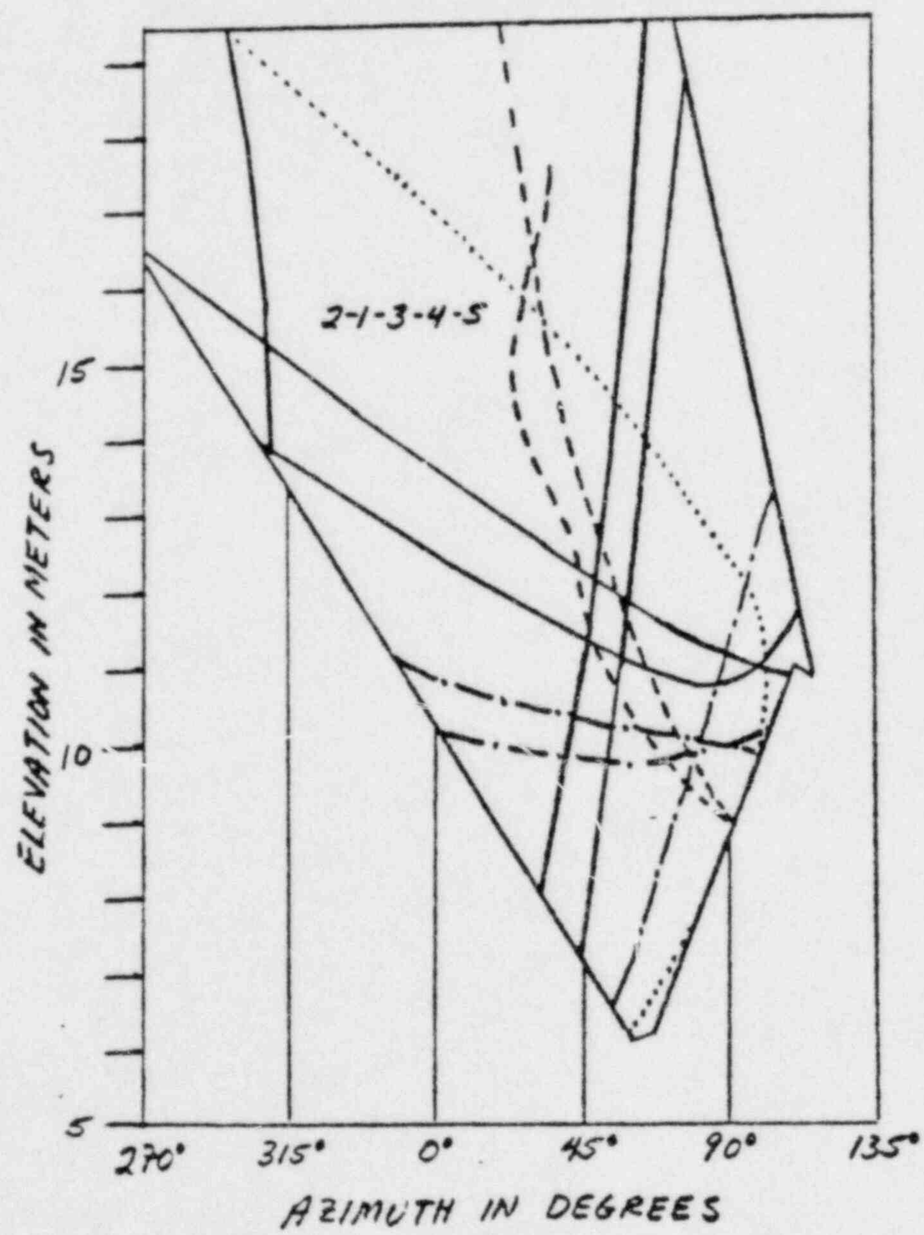

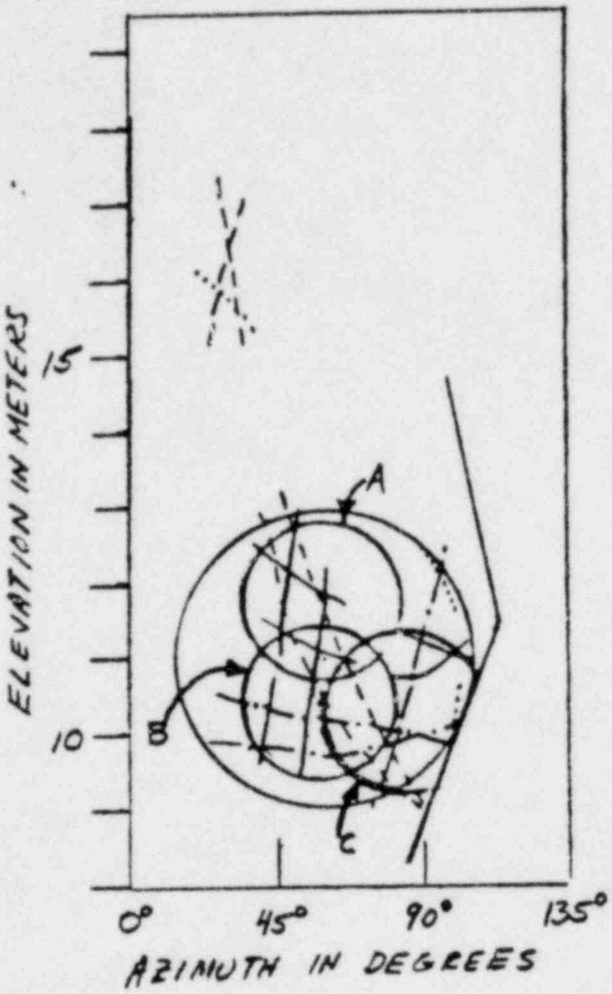

FIGURE 4. THE MOST PROBABLE ESTIMATE OF IMPACT POSITION AND THREE EQUALLY PROBABLE 2.5 m^2 ESTIMATES

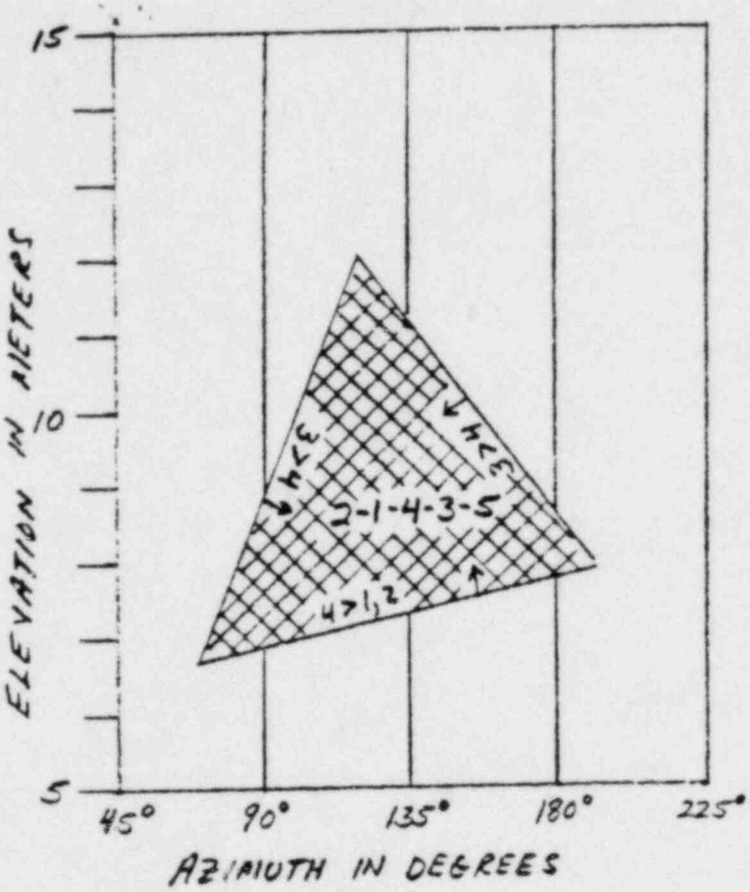

FIGURE 5. MOST PROBABLE ORDER ZONE FOR CASES #2 AND #3

2. Operator/computer interaction for abnormal condition control

HERL research personnel:
Y. Osawa
T. Watanabe

Activities: Design and implementation of advanced control and instrumentation systems emphasizing operator/computer interaction.

Conclusions: Figure 1 shows a schematic diagram of an advancement of the NUCAMM-80 control system that was investigated at HERL. This conceptualization is discussed in the following section of this report.

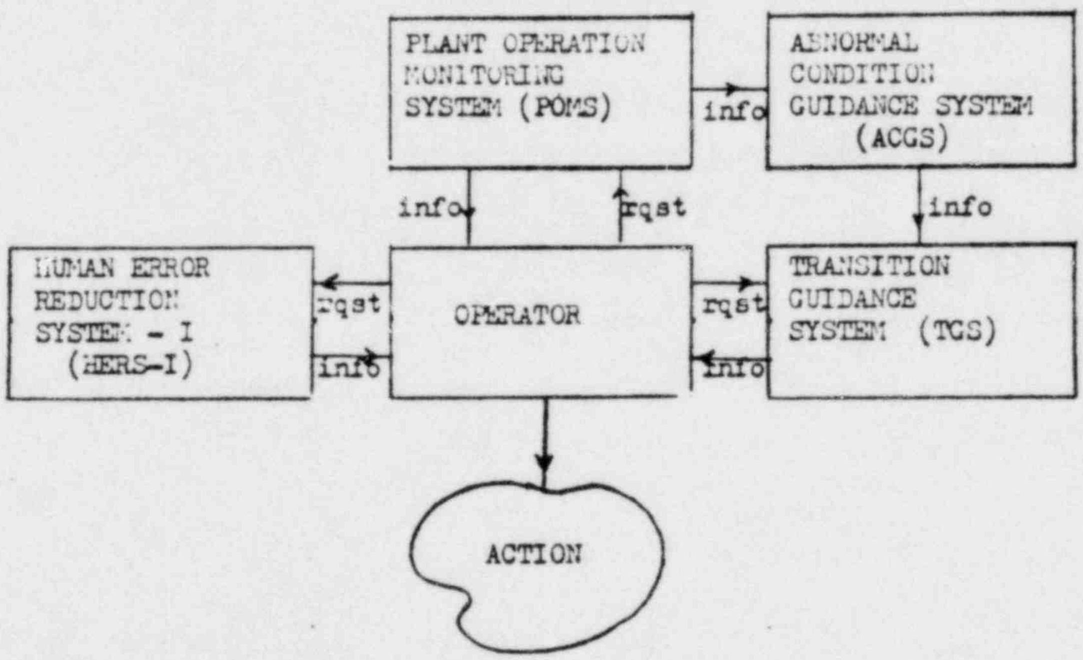

info = information flow
rqst = request for information

Figure 1. Schematic Diagram of Logical Arrangement for Operator Guidance System.

Background

The Energy Research Laboratory, Hitachi, Ltd. has an interest in computerizing a system for providing guidance to operational personnel of BWRs to avoid abnormal occurrences and to identify procedures to follow subsequent to the onset of an abnormal occurrence that will assist in mitigating potential serious consequences.*

Further study and analysis of the role of computer-based systems for operational guidance reveals that the hardware and elements of software for dealing with reduction of human errors and recovering from equipment failures are common. Also, many features of the current NUCAMM-80 system are well-suited for incorporation of this capability. The NUCAMM-80 Plant Operation Monitoring System (POMS) already has the following aims:**

(1) to detect anomalies of the plant at an early stage
(2) to give information on their causes and locations
(3) to give information on corrective actions.

Thus, a conceptualized system for providing guidance to operational personnel of BWRs to avoid abnormal occurrences and to identify procedures to follow subsequent to the onset of an abnormal condition represents logical continuing R&D directed toward enhancing the NUCAMM-80 system

---

In the United States, the Nuclear Regulatory Commission has determined*** that an on-site Technical Support Center be established at each operating reactor and be included in the design of future nuclear plants. This conclusion is based upon analysis of the events that occurred during the TMI-2 accident.

The principle mission of the Technical Support Center is to improve operational safety of nuclear plants through improved support of control room command and control functions. This mission is very similar to the mission of a computerized operator guidance system and it was concluded that the respective roles of these systems need to be understood in order to provide a framework for conceptualization of the proposed computer-based guidance system.

---

*Toshiba has also expressed interest in an "operator action guide", see e.g. H. Kawahara, et al., "On-Line Process Computer Application for Operator's Aid in Toshiba BWR," IAEA IWG/NPPCI Specialists' meeting 12/79, Munich

**K. Yamazaki et al., "Development of Plant Monitoring System for Nuclear Power Plants," IAEA, 12/79.

***"TMI-2 Lessons Learned Task Force Status Report and Short Term Recommendations," Office of Nuclear Reactor Regulation, USNRC, NUREG-0578, July 1979. "TMI-2 Lessons Learned Task Force Final Report," Office of Nuclear Reactor Regulation, USNRC, NUREG-0585, October 1979.

To help understand these roles, a descriptive scenario of control room key events and actions during the course of a generalized serious operational incident was developed. The parallel support activities expected to be provided by a realistic computerized guidance system and a technical support center are described in Table 1.

Stage I of the scenario outlined in Table I is premised on the assumption that a computerized system can sense the pre-event process variables and equipment configuration. The combination of signals from an unexpected event, automatic actions, and operator input can be logically related to an event classification that calls for a specific post-event configuration to be achieved. A computerized system can provide operational guidance to achieve the transition to the post-event configuration and to confirm that plant process variables are behaving according to expectations. It is assumed that in this early stage of an incident a technical support center provides no operational assistance.

The majority of incidents are terminated in Stage II and a computerized system can provide guidance to recover or secure the plant or a subsystem.

However, if additional unexpected events occur, the potential for providing adequate logic for a computerized guidance system becomes more speculative. Communication between operators and a computerized guidance system is shown in stage II but it is expected that if secondary events prolong the incident, the response will shift from reliance on procedures and training to more judgemental options. In this case, the technical support center begins to play an important role. If an incident continues to stage III then it is assumed that the types of actions to be taken are beyond the capability of a computerized guidance system and safety must rely on the coordinated judgement of operators and technical advisors.

Assumptions

A comprehensive background investigation has suggested that a computerized guidance system is developable to reduce human errors in normal operation and to enhance operator response following unexpected events. It is reasonable to require the computerized guidance system to be a significant aid in achieving prompt and effective configuration changes in aiding the operator to confirm the trahectory of plant process variables. If an incident progrsses beyond a level of complexity where responses can be pre-determined, then the operator will have to rely on a more judgemental system such as a technical support center for assistance. A truly adaptive computerized system may be feasible at some time in the future but this possibility is not explored here.

To be effective, the system should be highly conversational (between operator and computer) and should be in general use by the operator in normal operation as well as emergencies. So as not to impede prompt action, the computerized guidance system must operate at a speed that is compatible with the real time of events and operator decision time. This implies that detailed calculations and iterations are beyond the scope of

TABLE I

OPERATORS, COMPUTERIZED GUIDANCE SYSTEM, TECHNICAL SUPPORT CENTER DURING OPERATIONAL INCIDENTS

Stage of Incident	Approx. Time Interval	Operator (Control Room) Status/Events/Action	Computerized Guidance System Status/Events/Action	Technical Support Center Status/Events/Action
0	0 (minus)	Surveying Plant Status	Pre-event Plant Configuration Pre-event Plant Process Var's.	Stand by
I	0-1 minute	Unexpected Event(s) Auto Systems Activated Operator Surveillance Perceived Causes/Correction	Event Classification Desired Post-event Plant/System Configuration	Activate Plant Status Surveillance Activate Fault Detection Initiate Situation Tracking
		Strong reliance on procedures/training	Guidance to desired config. Guidance to confirm process var's.	
II	1-10 minutes	Procedures/training terminate incident	Guidance to recover or secure plant/system(s)	Evaluate minor incident
		or		
		Secondary events/some unexpected Auto systems cont. Potential causes identified Corrective actions identified	Event Classification Desired Post-event Plant/System Configuration	Initial Problem Analysis Identify causes Evaluate Corrective Action Severity Assessment
		Reliance on procedures/training and judgement	Guidance to desired config. Guidance to confirm process variables	Advice to operator
III	10-60 minutes	Assume incident not terminated Continued situation appraisal, corrective actions, severity assessment, notification/alert decisions	Beyond capability	Problem diagnosis Operational advice Alert Decisions Simulations Emergency mobilization Off-Site support
IV	60+ minutes	"	"	"

the guidance system. The guidance system should have fail-safe qualities so as not to mislead operators in an emergency or aggravagate an emergency situation. When optional control strategies exist, the guidance system should generally provide conservative instructions.

Conceptualization

For the sake of economy of organization, the conceptualized system is divided into several subsystems. The system to aid in reduction of human errors of the first type (operator action with incorrect or inconsistent previous action) is called HERS-I (Human Error Reduction System - 1). The system to reduce human errors due to omission of system tests, etc. is called HERS-II (not discussed in this report). A system to guide operators in achieving a transition from one operating state of the power plant or a subsystem of the plant is called TGS (Transition Guidance System). The system to provide guidance to operators following the development of an abnormal condition is called ACGS (Abnormal Condition Guidance System).

HERS-I Concept

The HERS-I is simply a computerized system to aid the operator in taking a contemplated action (e.g. open a valve, start a pump, etc.) and insuring that the action is consistent with prior actions. The procedure is imagined to be based on an interactive "pointing" device of a CRT screen. The resulting procedure is as follows:

HERS-I Screen	Operator
Continuously displays a diagram of the plant with major systems shown	Contemplates taking an action concerning a particular system. Selects system(s) affected by pointing on screen.
Displays selected system diagram	Selects subsystem(s) affected by pointing on screen.
Displays selected subsystem diagram	Selects component(s) affected by pointing on screen.
Displays component and list of possible operator actions	Selects action to be performed (pointing)
Produces check lists to permit action	Fulfills required checks and/or takes actions and enters this on display (pointing)
Display acknowledges fulfillment of required prior condition (perhaps changes itsm in check list from red to green)	Initiates contemplated action, enters fact to HERS-1
Resets and records	

TGS Concept

If the power station or a selected subsystem of the power station is operating in a given state, the operator is often required to cause a transition to a different state by altering the configuration of plant equipment. The classic transitions for the entire power station are start-up and shut-down. Load following is becomming increasingly important as nuclear plants grow in number to a larger fraction of the electrical grid. In each of these cases, a number of configuration changes in pumps, valves, control rods, etc. are required to make the transition. System transitions may involve switching to parallel equipment or changing the status of coolant inventory control during steady-state operation.

To explain the logic of transitions, three state vectors are defined. These are $\underline{P}$ (for plant), $\underline{E}$ (for equipment) and $\underline{S}$ (for system). The $\underline{P}$ state vector has components that may vary continuously. These components are equal to the values of plant process variables such as steam flows, pressures, power, temperature, etc. This vector may be denoted by $\underline{P} = (P^1, P^2, \ldots P^N)^T$. The $\underline{S}$ vector is similar to the $\underline{P}$ vector but restricted to the state variables of a particular system of the plant. For example, $\underline{S} = (S^1, S^2, \ldots S^N)^T$ for the feedwater system may consist of suction, flow, etc. of feedwater pumps. The $\underline{E}$ vector is thought to consist of two kinds of components. The majority are binary and represent the states such as "on" and "off", "open" and "closed", etc. Some elements of the $\underline{E}$ vector may be continuous for "CRD position", "Turbine Control Valve Position", and other equipment variables that may take on a continuum of values.

In the language of these three vectors, any plant operating state may be described by a set of such vectors. For example, let $\underline{P_0}$, $\underline{E_0}$, $\underline{S_{i0}}$ ($i = 1,2,\ldots L$), $\underline{E_{ik0}}$($k = 1,2,\ldots K_i$) represent an operating state of the plant and key equipment ($\underline{P_0}$, $\underline{E_0}$) and L systems for which the i^{th} system has an equipment configuration ($\underline{S_{i0}}$, $\underline{E_{ik0}}$).

$\underline{P_0} = (P_0^1, P_0^2, \ldots P_0^N)^T$ is a vector of the values of N plant process variables in the "0" operating state.

$\underline{E_0} = (E_0^1, E_0^2, \ldots E_0^M)^T$ is a vector of M equipment states for major components affecting plant process variables in the "0" state.

$\underline{S_{i0}} = (S_{i0}^1, S_{i0}^2, \ldots S_{i0}^{I_i})^T$ is a vector of I_i elements for system i describing the state variables of the system in the "0" state.

$\underline{E_{ik0}} = (E_{ik0}^1, E_{ik0}^2, \ldots E_{ik0}^{J_{ik}})^T$ is a vector of J_{ik} values for the equipment configuration of the k^{th} type of equipment in system i describing the equipment states in the operating "0" state.

- - - - - - - - - - - - - - - -

Let us assume that an operator is required to cause the plant to make a transition from the current operating state $\underline{P_0}$ to a new (desired) operating state $\underline{P_D}$. Let $\underline{\underline{F_{0D}}}$ be the (mathematical) operator applied to $\underline{P_0}$ to produce the vector $\underline{P_D}$, i. e.

$$\underline{P_D} = \underline{\underline{F_{0D}}} \left\{\underline{P_0}\right\}$$

Now, to cause this transition, the operator (human) does not directly control $\underline{\underline{F_{0D}}}$. Instead, he varies $\underline{E}$ vectors by control actions.

Let $\underline{\underline{G_{0D}}}$ be the control action applied to the initial operating state to produce the equipment configuration of the finally desired operating state. Then, we write

$$\underline{E_D} = \underline{\underline{G_{0D}}} \left\{\underline{E_0}\right\}$$

In a similar way, if the transition of a system from $\underline{S_{i0}}$ to $\underline{S_{iD}}$ is required, the (human) operator controls $\underline{E_{ik}}$ and this can be described by the (mathematical) operator $\underline{\underline{G_{ikOD}}}$. Of course, it is possible that $\underline{S_{i0}} = \underline{S_{iD}}$ even though $\underline{E_{ik}}$ is changed. (For example, a parallel pump may be substituted with the result that the process variables before and after the substitution are the same.)

Let the transition in a system state vector be denoted by $\underline{\underline{H_{iOD}}}$ and in the equipment configuration as $\underline{\underline{G_{ikOD}}}$. A transition to the desired (D) state of system and equipment, respectively, is then denoted by

$$\underline{S_{iD}} = \underline{\underline{H_{iOD}}} \left\{ \underline{S_{i0}} \right\}$$

$$\underline{E_{ikD}} = \underline{\underline{G_{ikOD}}} \left\{ \underline{E_{ik0}} \right\} \quad (k = 1,2, \ldots J_{ik})$$

Now, the (human) operator action is contained in $\underline{\underline{G_{ikOD}}}$. In general, an action may affect one equipment item per action so the $\underline{\underline{G_{ikOD}}}$ matrix is considered to be diagonal and (often) consisting only of binary elements.

As an example, consider the $\underline{E_{ik}}$ vector to represent components of the feedwater system. For economy of notation, the "ik" subscript is dropped in this example. The feedwater system pumps are represented in this example as follows:

E^1 = state of TDRFP-A (1 = operating, 0 = shut down)
E^2 = state of TDRFP-B (1 = operating, 0 = shut down)
E^3 = state of MDRFP-A,B (1 = operating, 0 = shut down)

In normal operation, the feedwater pump line-up is

$$\underline{E_0} = \begin{pmatrix} 1 \\ 1 \\ 0 \end{pmatrix} .$$

In case of a failure of TDRFP-A, the desired state of the equipment in the feedwater system is

$$\underline{E_D} = \begin{pmatrix} 0 \\ 1 \\ 1 \end{pmatrix}$$

Now, $\underline{\underline{G_{OD}}}$ may consist of three types of elements, "1, 0, N". The operation of an element of $\underline{\underline{G}}$ on an element of $\underline{E}$ is defined such that this operation is binary addition without carry for the "1" and "0" elements and "no operation"for the "N" element. That is,

$$1(0) = \frac{\begin{matrix}0\\1\end{matrix}}{1} \qquad 1(1) = \frac{\begin{matrix}1\\1\end{matrix}}{0}$$

$$0(0) = \frac{\begin{matrix}0\\0\end{matrix}}{0} \qquad 0(1) = \frac{\begin{matrix}1\\0\end{matrix}}{1}$$

$$N(0) = \text{no op} \qquad N(1) = \text{no op}$$

In the above cases, the operator 1( ) implies a transition and the operator 0( ) implies no transition. The element N of the $\underline{\underline{G}}$ matrix is taken to result in a null (meaning that there is no such operation defined).

The transition in feedwater equipment is then written as

$$\begin{pmatrix} 0 \\ 1 \\ 1 \end{pmatrix} = \begin{bmatrix} 1 & N & N \\ N & 0 & N \\ N & N & 1 \end{bmatrix} \begin{pmatrix} 1 \\ 1 \\ 0 \end{pmatrix} \quad (\underline{E_D} = \underline{\underline{G_{OD}}}\ \underline{E_O})$$

This equation can be interpreted by discussing the meaning of several elements. Element G_{11} is the control action to be applied to TDRFP-A to affect the operation of TDRFP-A. To achieve the transition desired, the action is 1( ). Since the initial operating state of the feedwater pump TDRFP-A is "1" (meaning that it is operating) the operation results in the first element of $\underline{S}$ being changed from "1" to "0". Or, in plain language, the operation is read as "turn off TDRFP-A". Element G_{12} is the control action to be applied to TDRFP-A to affect the operation of TDRFP-B. Since no such control action is possible, the element, and all other off-diagonal elements, is "N". Element G_{22} is the control action to be applied to TDRFP-B to affect TDRFP-B. The operator for the transition is O( ) resulting in the second element of the $\underline{S}$ vector remaining as a "1". Again, in plain language, this operational notation means "leave TDRFP-B running".

For this example, the initial operating state of the feedwater equipment is $\underline{E_0} = (1, 1, 0)^T$. The process variables of the feedwater system in this state are $\underline{S_0}$ (whose structure is discussed later) and the overall plant process variables are $\underline{P_0}$. Because of some failure in TDRFP-A the transition

$$\underline{E_D} = \underline{\underline{G_{OD}}} \{\underline{E_0}\}$$

is called for where

$$\underline{\underline{G_{OD}}} = \begin{bmatrix} 1 & N & N \\ N & O & N \\ N & N & 1 \end{bmatrix}$$

Note that $\underline{\underline{G_{OD}}}$ is a transition operator. It could also be thought of as a "guidance operator" from the current operating state of equipment in the feedwater system to the desired operating state of feedwater equipment. Namely, $\underline{\underline{G_{OD}}}$ describes the guidance that an operator should receive to make the desired transition. (It is no accident that the nomenclature of this operator closely resembles GOD!)

\- - - - - - - - - - - - - - - - - - - -

During a typical transition from one state to another, the operator performs two functions. These are

(1) Control action to affect the transition

(2) Surveillance and confirmation of the response of system variables to the action performed.

These can be described in terms of the quantities defined above.

Suppose the operator desires to cause a transition from a current operating state of the plant $\underline{P_O}$ to a desired operating st $\underline{P_D}$. To accomplish this transition, he must take a series of actions affecting plant equipment. These actions imply that the state variables of systems within the plant are changed.

The operator (and/or automatic systems) make a series of transitions (in some order)

$$\underline{E_D^m} = \underline{\underline{G_{OD}^m}} \left\{ \underline{E_O^m} \right\} \quad (m = 1,2,\ldots)$$

that result in system state transitions

$$\underline{S_D^m} = \underline{\underline{H_{OD}^m}} \left\{ \underline{S_O^m} \right\} \quad (m = 1,2,\ldots).$$

Clearly, the law $\underline{\underline{H_{OD}^m}}$ describing the state transitions of systems is a function of the $\underline{\underline{G_{OD}^m}}$ that are taken; so, more explicitely

$$S_D^m = \underline{\underline{H_{OD}^m}} \, (\underline{\underline{G_{OD}^m}}) \left\{ \underline{S_O^m} \right\}$$

The plant process variables are related to the transitions in state variables of systems and the plant then makes a transition to state $\underline{P_D}$ by the rule

$$\underline{P_D} = \underline{\underline{F_{OD}}} \, (\underline{\underline{H_{OD}^m}}) \left\{ P_O \right\} \quad \text{(all m)}$$

- -

We are now in a position to define the mechanics of a TGS (transition guidance system).

First, such a hypothetical system should be capable of sensing the current state of the plant as well as the state of subsystems in the plant. That is, the TGS should be capable of continuously sensing $\underline{P}$ and $\underline{S}$.

Second, the TGS should be capable of receiving specifications for the state variables of a desired state. That is, the system should be able to receive messages that enable it to determine the state variables of $\underline{P}_D$ and/or $\underline{S}_D$.

Third, the system should have a logical structure that will generate a set of guidance matrices $\underline{\underline{G}}^m_{OD}$ that cause equipment transitions resulting in $\underline{P}_0 \rightarrow \underline{P}_D$ and $\underline{S}_0 \rightarrow \underline{S}_D$. These transition rules must be reported to the operator.

The TGS at this stage is capable of providing guidance to an operator on the actions to take to cause the desired transitions.

As actions are taken, the TGS should sense $\underline{P}$ and $\underline{S}$ and compare these values with expectations in order to aid the operator in his surveillance and confirmation role. That is, the TGS should have simulation capability. This means that the expected trajectories of $\underline{S}$ and $\underline{P}$ should be reported to the operator and compared to the sensed values of $\underline{S}$ and $\underline{P}$. In particular, discrepancies between expectations and true performance should be highlighted. To accomplish this task, the TGS must have the capability of generating $\underline{\underline{H}}^m_{OD}$ $(\underline{\underline{G}}^m_{OD})$ and $\underline{\underline{F}}_{OD}$ $(\underline{\underline{H}}^m_{OD})$ for all m.

In addition to TGS, the operator can make use of HERS-I and HERS-II to accomplish a transition. When the operator receives guidance from TGS to take an action, he can refer to HERS-I for the necessary checks and tests required to allow the action. A transition to a new operating state may require the performance of certain special tasks. These can be communicated to the operator and/or maintenance personnel by HERS-II.

ACGS Concept

The abnormal condition guidance system (ACGS) is conceived as a logic element that provides input to the TGS. In this case, the TGS is capable of responding to an initiation from the ACGS instead of from the operator. The TGS is capable of sensing the state of plant process variables, $\underline{P}$, of system variables, $\underline{S}$, and equipment configuration, $\underline{E}$. An abnormal condition is sensed by the ACGS by sensing changes in $\underline{P}$ or $\underline{S}$ that are unrelated to expected changes due to operator action. The ACGS must have logic that, upon sensing such a change, will evaluate it in terms of the desired state of plant and system operation. This means that the ACGS must generate desired states $\underline{P_D}$ and $\underline{S_D}$. To achieve these desired states, it is necessary to make transitions in the equipment configuration, $\underline{E}$. This is done according to the guidance $\underline{G}$ supplied by the TGS in response to the input concerning the desired state after an abnormal occurrence generated by ACGS.

For example, suppose that the suction flow of the TDRFP-A decreases and is sensed. The initial configuration of $\underline{E}$ for this case is $\underline{E} = (1,1,0)^T$. The decrease in reactor water level accompanying this feedwater flow reduction is also sensed. The initial plant and feedwater system operating state variables were $\underline{P_0}$ and $\underline{S_0}$ respectively. In this case, ACGS logic evaluates the desired end states to be $\underline{P_D} = \underline{P_0}$ and $\underline{S_D} = \underline{S_0}$. To achieve this, the required transition in feedwater equipment is

$$\underline{\underline{G_{OD}}} = \begin{bmatrix} 1 & N & N \\ N & 0 & N \\ N & N & 1 \end{bmatrix}$$

as before. Thus the logic of ACGS, coupled with TGS, generates this transition matrix and reports "guidance" to the operator.

In this case, the action specified by element G_{11} operating on element E_1 (1(1)=0) for TDRFP-A must generate an instruction of the form "Manually trip TDRFP-A". Since when TDRFP-A is manually tripped, MDRFP-A,B are automatically started, the guidance message for this component of the transition must be of the form "Verify start of MDRFP-A,B". This message is generated from element G_{33} operating on E_3 (1(0)=1).

Perhaps the operator should also be prompted to monitor the flow of the feedwater system. The ACGS/TGS should generate expected trajectories of at least the feedwater flow and reactor water level for a normal transition of this type. A message to the operator to verify that feedwater flow and water level recover can be generated. ACGS/TGS may track the difference between $\underline{P}$ and $\underline{P_D}$, $\underline{S}$ and $\underline{S_D}$. In normal situations, recovery will be complete and the scene of the action changes to the recovery of the operational status of TDRFP-A.

After maintenance, a transition from the $(0,1,1)^T$ state to the $(1,1,0)^T$ state of $\underline{E}$ (feedwater equipment) can be assisted by TGS.

However, assume that MDRFP-A,B fail to start or fail to provide feedwater flow for some other reason. In this case, $\underline{P}$ continues to diverge from $\underline{P_D}$. If the water level decreases sufficiently, an auto or manual scram may be called for. In a scram the operator is normally required to take several actions to secure plant equipment and is expected to survey plant variables for expected behavior. The new desired state is a shut down state. This is sensed by ACGS and operator action and surveillance instructions are generated by TGS.

If still more unexpected events such as the failure of a valve to operate or the failure of the scram system to actuate occur, then the ACGS/TGS may be unable to provide adequate guidance and the decisions on proper action may shift to operator judgement supplemented by technical advice from the technical support center.

The more likely sequence of events is that further abnormal occurrences do not complicate the scenario. In this case, the scram procedes as anticipated. It is again plausible that HERS-I will come into action to provide ch ck lists for certain operator actions. HERS-II may be required since many special tests and checks are normally required to recover from a scram.

Conclusions

The conceptualization discussed above implies a schematic operational diagram shown in fig 1. The operator, while making routine control actions, consults HERS-I to check that the action is in procedural conformance with previous actions. When transitioning from one operating state of the plant or a subsystem to another, the operator consults TGS for procedures to accomplish the transition. The operator normally monitors POMS and, in addition, is provided with simulations of the expected trajectory of plant and system process variables by TGS.

In this configuration, dialog between the operator and HERS-I, TGS are routine and relatively continuous. Therefore, the operator gains familiarity with HERS-I and TGS through normal operation.

In an abnormal occurrence, the operator is presented with information by POMS and the ACGS logic generates a desired state transition on the basis of POMS information. This triggers TGS to report these transition instructions to the operator. In this case, the operator can easily recognize the abnormal condition guidance to follow because of continual experience with the system. Also, experience with HERS-I should aid the operator in the avoidance of inappropriate actions. After transition to a new state is complete and the abnormal condition is corrected, HERS-II (not shown in the logical diagram because it is logically separated from the operator's direct responsibility) is of value in assuring that necessary tests, checks, and maintenance are performed.

If the abnormal condition progresses beyond the capability of the procedures and training of the operator as well as the ability of the ACGS/TGS to provide operational guidance, then it is necessary to call upon additional technical assistance. This can be provided by advisors from the technical support center whose analysis of the plant situation will be augmented by the record of actions by the ACGS and the past guidance provided by TGS. Also the discrepancies between expected trajectories produced by TGS and those actually experienced will be of value in analyzing the abnormal situation. It is expected that an enhanced technical support center will have simulation capability. The design and operation of the less sophisticated simulations associated with the TGS should be of significant value for technical support center design and for analyzing the causes and potential consequences of a sequence of abnormal occurrences that may proceed beyond the capability of the ACGS/TGS.

- - - - - - - - - - - - - - - - - - -

3. BWR transient and stability calculations

HERL research personnel:
H. Motoda
O. Yokomizo

Activities: Development of a computer code with coupled neutronics/thermal-hydraulics to calculate the time dependent transient behavior of BWRs for various disturbances is well advanced.

Conclusions: HERL has developed a time domain stability code for BWRs that has the capability of handling parallel channel effects. At present this code uses point neutronic kinetics but a multi-dimensional, time-dependent FLARE model for neutron kinetics is nearly complete.

In analyses of a commercial size BWR it was found that a smaller decay ratio than the current design code resulted. A nonlinear effect tending to increase decay ratio with decreased amplitude was observed. The parallel channel effect is manifested by a less stable core and phase shift between power and pressure.

Summary of Current (6/80) results

(1) Copy of recent ANS paper

(2) Copy of presentation slides

(3) Time-dependent FLARE

The formulation of a multi-dimensional, time-dependent FLARE code is complete. The formalism carefully takes boundary effects and the calculation of the adjoint into account. Coding of this model is nearly complete.

7. J. R. REAVIS, "Vibration Correlation for Maximum Fuel-Element Displacement in Parallel Turbulent Flow," *Nucl Sci. Eng.*, **38**, 63 (1969).

2. Development of a Time-Domain BWR Core Stability Analysis Program, *Osamu Yokomizo, Isao Sumida, Hiroshi Motoda (Hitachi/ERL-Japan)*

In the operation of a boiling water reactor (BWR) at partial power and lower core flow, the nuclear thermal-hydraulic stability of the core is an important constraint and it has to be assured prior to operation that certain stability criteria are satisfied in all operating conditions.

Widely adopted computer programs to predict the core stability are those in the frequency-domain with parallel channel capability or those in time-domain that treat the core as a single channel. The frequency-domain approach is very useful for the practical design purpose because of the short computation time to predict conditions for the inception of instability. However, for more realistic design, analyses of the transient behavior of the core with respect to the system nonlinearity are desirable. Parallel channel effect is also regarded to be important in core stability analysis. To satisfy these requirements, a time-domain program with parallel channel capability has been developed.

This program takes into account the following phenomena of the BWR core:

1. neutron kinetics with Doppler and void reactivity feedback
2. fuel heat transfer
3. thermal hydraulics of coolant in parallel fuel channels
4. recirculation flow hydrodynamics.

Because of the nonlinearity and the large number of the system variables it was anticipated the program would consume a long computation time. Therefore, several assumptions and approximations were introduced for each of the models.

1. *Neutron Kinetics:* The point neutron kinetics model with prompt jump approximation was used. Reactivity is obtained by averaging the infinite multiplication factor with weighting of squared power level and correcting it with initial condition leakage.

2. *Fuel Heat Transfer:* Axial heat conduction was ignored and radial one-dimensional (1-D) equations were implemented. Temperature dependence of thermal conductivity was accounted for.

3. *Channel Thermal Hydraulics:* The following assumptions were applied to the 1-D separated flow model:

a. System pressure is uniform and varying by time.

b. Vapor is always at saturated condition.

c. Fluids are incompressible.

d. Flow quality in the subcooled boiling region is a smooth function of mixed quality.

With these assumptions, a unified expression can be used for all of the single phase, subcooled, and bulk boiling regions.

4. *Recirculation Hydrodynamics:* Energy loss and deposition in the recirculating flow were neglected. A 1-D momentum equation was used for calculating the pressure difference between core inlet and exit.

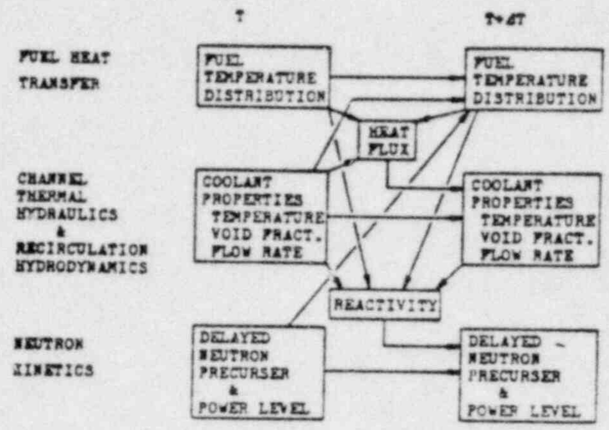

Fig. 1. Time integration scheme.

The implicit method was used to derive the finite difference equations for each model. The time-integrating scheme is illustrated in Fig. 1. First, fuel temperature distribution at time $t + \Delta t$ is calculated from temperature distribution, coolant properties, and power level at t. Heat flux during time interval Δt is then calculated from coolant properties at t and $t + \Delta t$. Using this heat flux, coolant properties at $t + \Delta t$ can be obtained. Next, average reactivity is calculated from fuel temperature and void fraction at t and $t + \Delta t$. Delayed-neutron precurser levels at $t + \Delta t$ are calculated using the average reactivity, and power level is obtained using the reactivity at $t + \Delta t$.

This program has been applied to a BWR/4 core under a natural-circulation condition. Figure 2 shows an example of the analytical results. The curves are responses of core power to sinusoidal variations of core pressure with the amplitude of 0.2 MPa and two different periods. It should be noted that in the 1-Hz case the response is not sinusoidal. It has been found from detailed examination that in this case

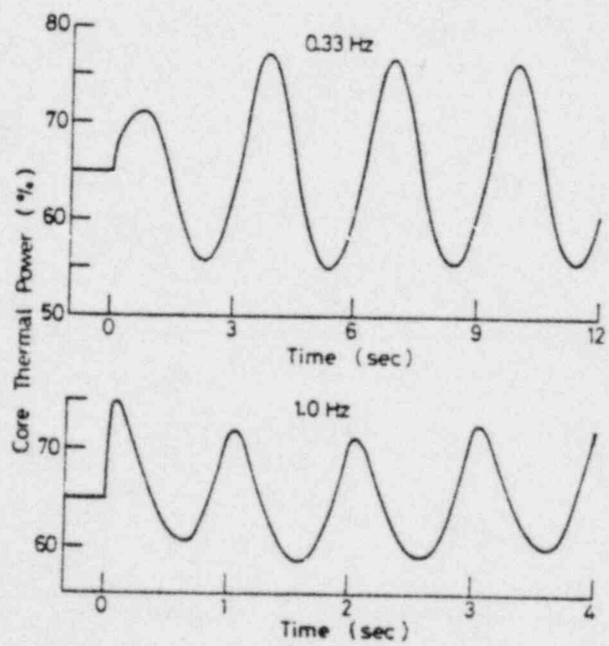

Fig. 2. Effect of nonlinearity and parallel channel geometry.

the central fuels and the peripheral fuels are behaving out of phase with each other, decreasing the change of the core reactivity, thus, the importance of nonlinearity and parallel channel effect has been demonstrated. This program is expected to be very useful in developing a new stability criterion.

3. An Advanced Absorber Assembly Design for Breeder Reactors, *A. L. Pitner, K. R. Birney (Westinghouse Hanford)*

An absorber assembly design has been developed that offers substantial improvements in performance characteristics and fabrication economics of breeder reactor control elements. The design represents a marked departure from conventional assembly configurations, including incorporation of large-diameter vented absorber pins, circular pin arrays and duct tubes, and advanced alloy structural components. Benefits achievable from application of this advanced design include faster scram time, longer assembly lifetime, and reduced fabrication cost.

The principal design changes adopted in evolving from the Fast Flux Test Facility (FFTF) reference absorber assembly design to the advanced design are depicted in Fig. 1. Whereas the reference design is comprised of 61 sealed boron carbide pins arranged in a hexagonal configuration, the advanced design incorporates 19 vented pins arrayed in a circular pattern inside round duct tubes. Also, in lieu of AISI Type 316 stainless-steel reference duct and cladding material, the advanced design makes use of the advanced alloy D9 in the fabrication of these structural components. These design changes lead to a number of improvements in both performance and economics.

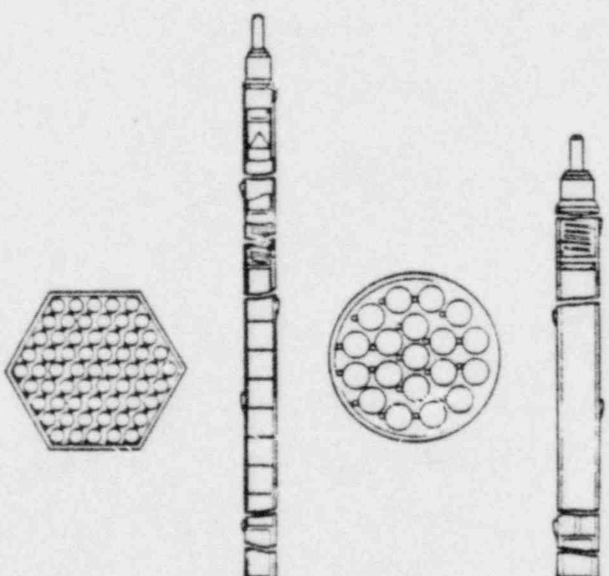

Fig. 1. Comparison of FFTF reference and advanced absorber assembly designs.

The boron carbide absorber material in breeder reactor control rods produces helium gas under irradiation service conditions. In sealed pins, the associated gas pressure buildup and high cladding stresses that develop can ultimately limit the absorber assembly lifetime. These problems are circumvented by venting the helium to the reactor coolant. In the present design, this is accomplished using a vent assembly comprised of a porous plug flow restrictor device located above a diving bell chamber at the bottom of the absorber pin. The porous plug is fabricated from sintered stainless-steel powder, and allows venting to occur only above some threshold pressure differential. The diving bell chamber serves to prevent sodium wetting of the porous plug. This vent assembly design was selected on the basis of suppressing sodium ingress to the absorber pin.

The transition from a 61-pin bundle design to a 19-pin bundle design offers substantial savings in fabrication costs. The pin diameter has been increased from 0.474 in. (1.204 cm) for the reference design to 0.784 in. (1.991 cm) for the advanced design. Since little gas pressure buildup occurs, the cladding wall thickness has been reduced from 0.051 in. (0.130 cm) to 0.025 in. (0.064 cm). The overall reduction in cladding volume makes additional space available for absorber material, and the ^{10}B content for the advanced design is 12.5% greater than for the reference assembly.

The advanced design employs round duct tubes, with hexagonal load pads affixed where the assembly mates with surrounding core assemblies. Whereas the torque imparted by the control rod drive mechanism during rod withdrawal can cause contact between the inner and outer ducts in a hexagonal design, round duct tubes will not interact under these circumstances. Thus, potential wear problems are avoided by employing a round assembly design. Another benefit gained with the round design is increased coolant flow through the pin bundle. The pin bundle/bypass annulus flow ratio for the hexagonal reference design is 60%/40%, while for the advanced design it is improved to 75%/25%.

The primary benefit gained in application of the advanced alloy D9 for structural components is related to assembly bowing behavior. With Type 316 SS, thermal and flux gradients across absorber assemblies result in significant bowing, which can lead to vertical travel interference and shortened lifetimes. D9 exhibits very low in-reactor swelling, which effectively eliminates problems related to duct bowing.

Scram performance of the advanced assembly is substantially improved relative to the reference design. The advanced assembly weighs less and exhibits reduced hydraulic resistance when compared to the reference design. Consequently, it responds faster to accelerating scram forces. Based on calculations performed using the SCRAM code,[1] which was developed for FFTF control rod scram analysis, the advanced absorber assembly scrams 30 to 40% faster than the reference assembly.

The FFTF reference absorber assembly design has been modified to increase its lifetime from 300 to 600 full power days (FPD). Lifetime analyses performed for the advanced design using the CONROD code[2] indicate that this assembly is capable of a 900-FPD lifetime in the FFTF. The 50% increase in design lifetime combined with reduced fabrication costs provide for substantial economic gains when the advanced absorber assembly is implemented in FFTF. Two of the absorber assemblies in FFTF will be replaced with advanced prototypes in the future to verify performance capabilities.

It is expected that the general benefits derived from the advanced absorber design developed for FFTF can be

Development of a Time Domain BWR Core Stability Analysis Program

INTRODUCTION

CURRENT METHOD -------- FREQUENCY DOMAIN

STABLE OR NOT, DECAY RATIO

MOST TIME DOMAIN CODE --- SINGLE CHANNEL

PURPOSE OF STUDY

1. DEVELOP A TIME DOMAIN CODE WITH PARALLEL CHANNEL CAPABILITY
2. INVESTIGATE EFFECT OF PARALLEL CHANNEL

ANALYTICAL MODEL

FUEL THERMAL HYDRAULICS

- FEW PARALLEL CHANNELS
- SPATIALLY UNIFORM PRESSURE (⇨MATERIAL PROPERTY)
- 1-D SLIP FLOW MODEL / QUASI-EQUILIBRIUM SUBCOOLED VOID

NEUTRON KINETICS

- 1 POINT MODEL WITH 6 DELAYED NEUTRON GROUPS
- PROMPT JUMP APPROX.

FUEL HEAT TRANSFER

- RADIALLY 1-D DISTRIBUTED PARAMETER MODEL

RECIRCULATION HYDRODYNAMICS

- INCOMPRESSIBLE FLUID IN 1-D FLOW PATH

RELATIONS AMONG VARIABLES

(HOW TO OBTAIN VARIABLES AT T+ΔT FROM THOSE AT T)

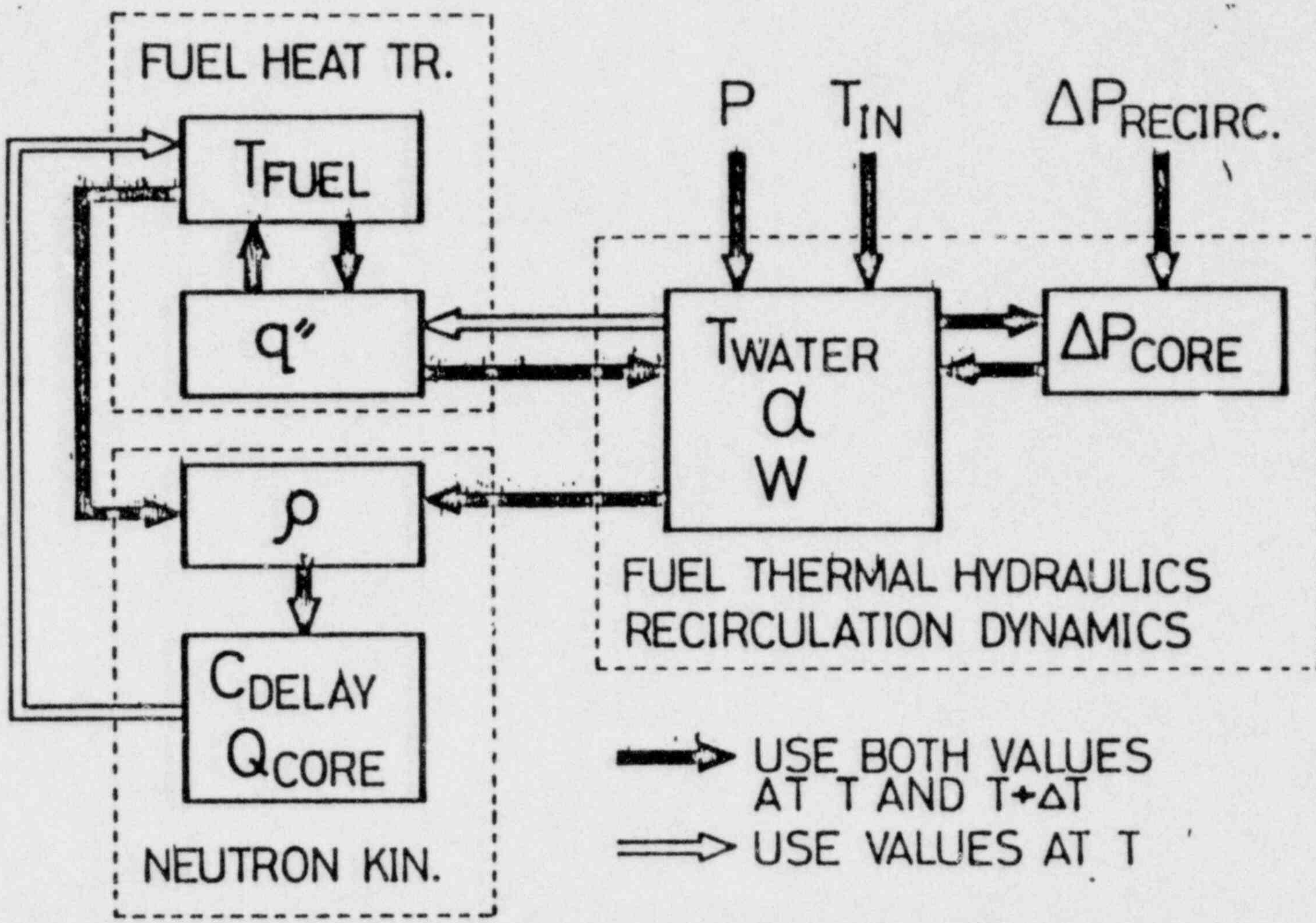

ANALYZED CORE

CORE FEATURES

RATED POWER	2381	MWT
RATED CORE FLOW	8335	KG/S
RATED PRESSURE	7.14	MPA
NUMBER OF FUEL BUNDLES	548	

DIVISION OF CORE

CHANNEL 1 (CENTRAL/HIGH POWER)	298	BUNDLES
CHANNEL 2 (CENTRAL/LOW POWER)	174	BUNDLES
CHANNEL 3 (PERIPHERAL)	76	BUNDLES

INITIAL CONDITION

CORE POWER	65	%
CORE FLOW	32	%
INLET TEMPERATURE	264	°C

CORE POWER RESPONSE TO SINUSOIDAL PRESSURE PERTURBATION

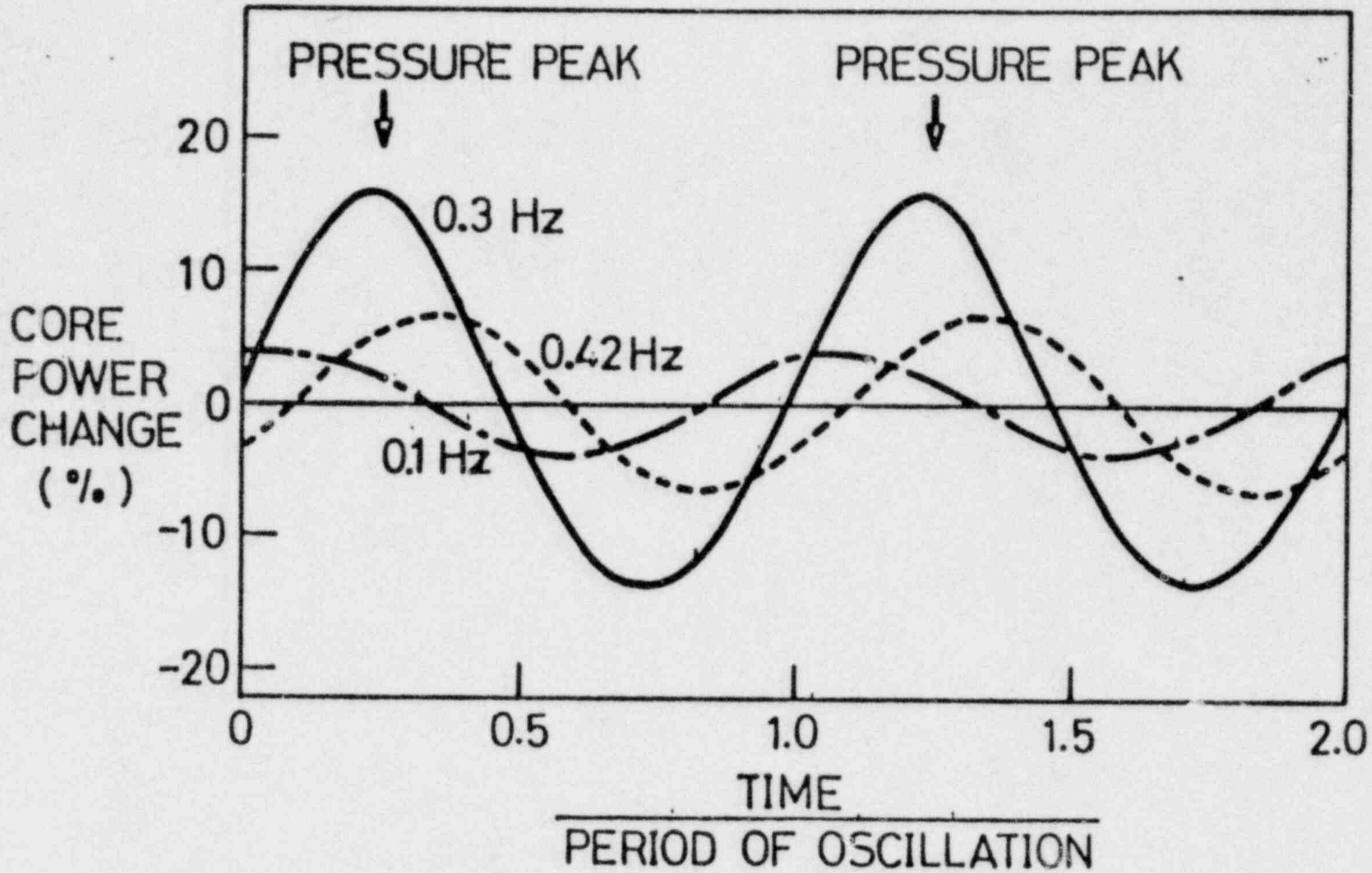

FREQUENCY RESPONSE OF POWER TO PRESSURE

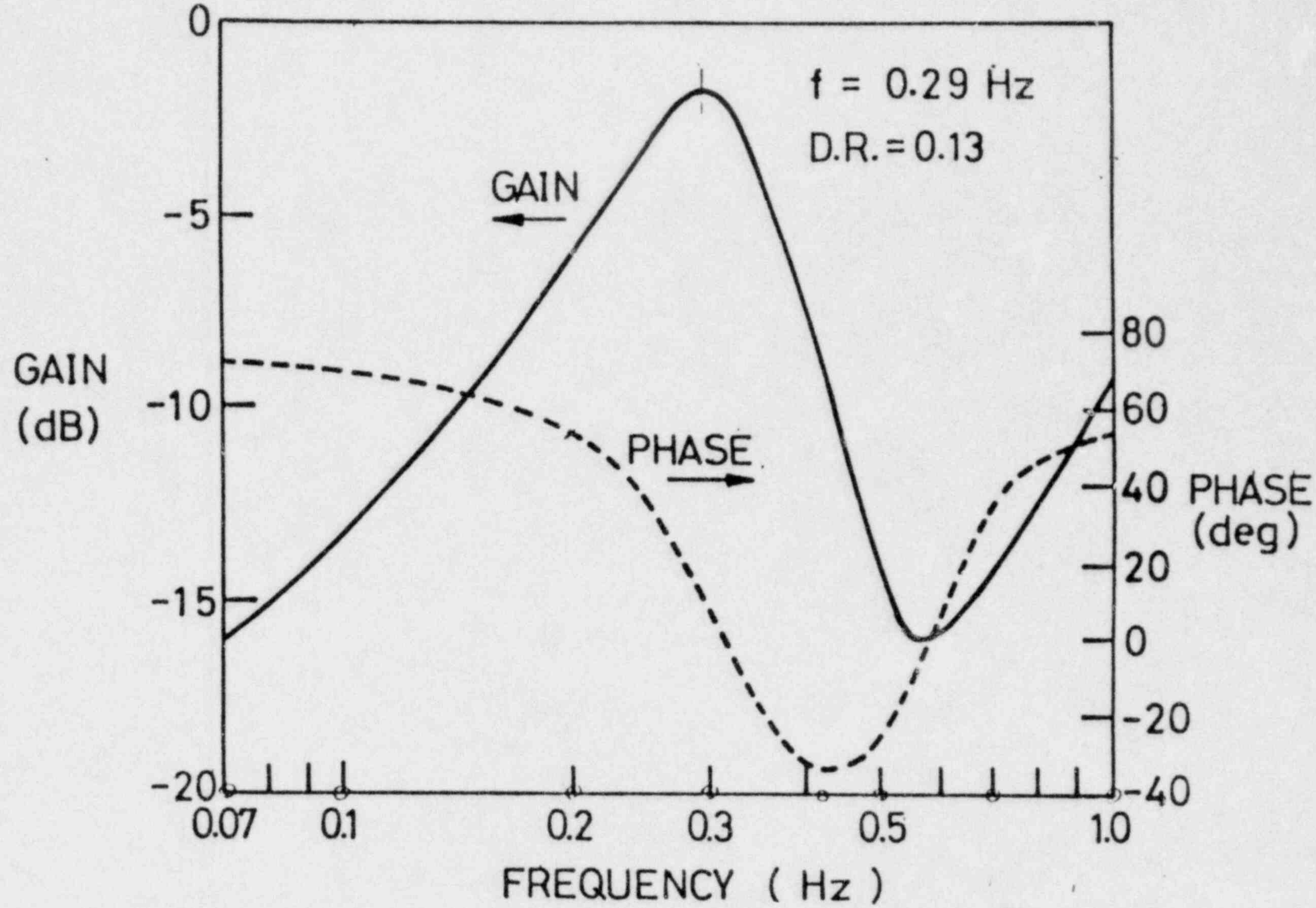

DIRECT CALCULATION OF DECAY RATIO

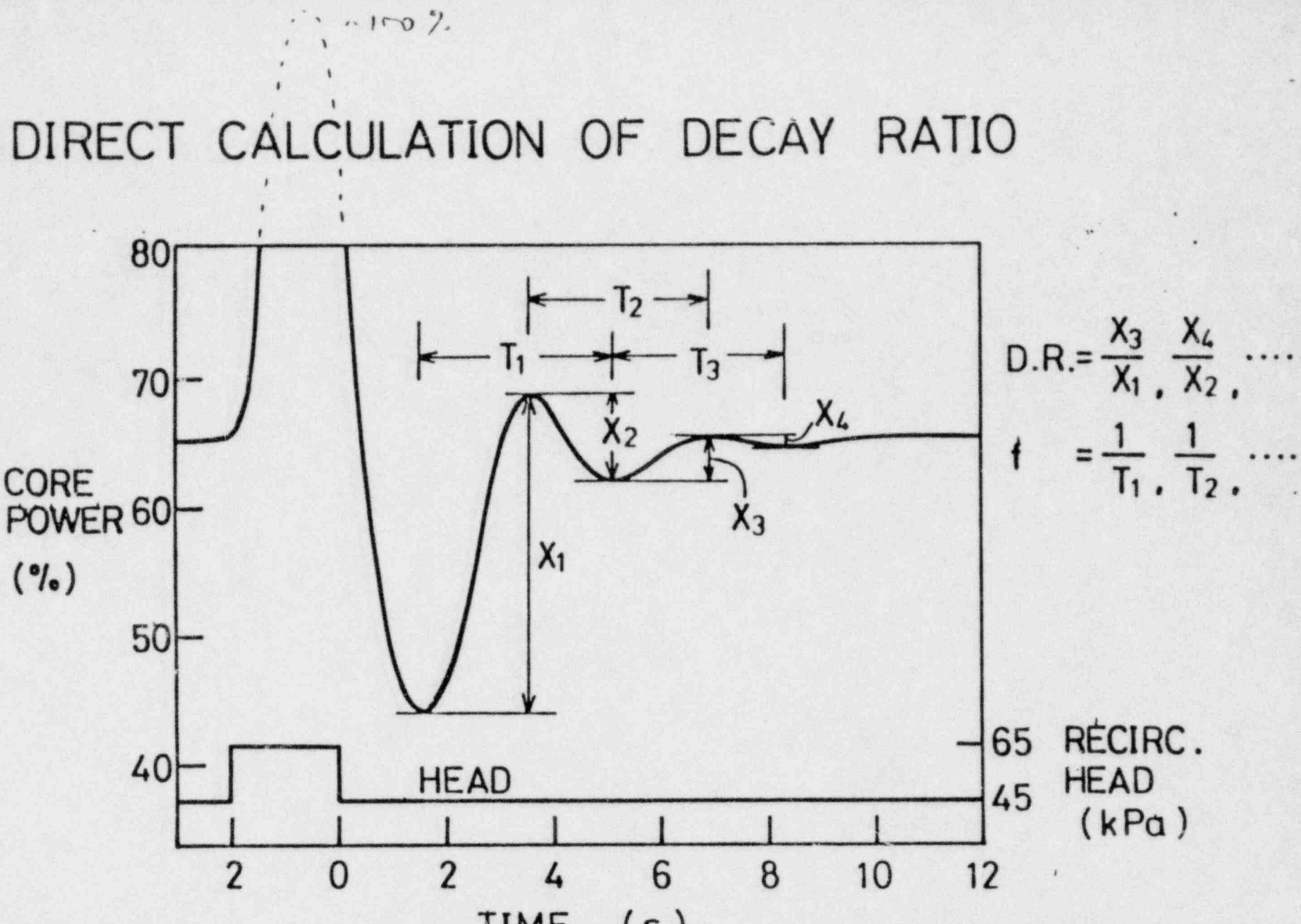

DECAY RATIO AND RESONANT FREQUENCY

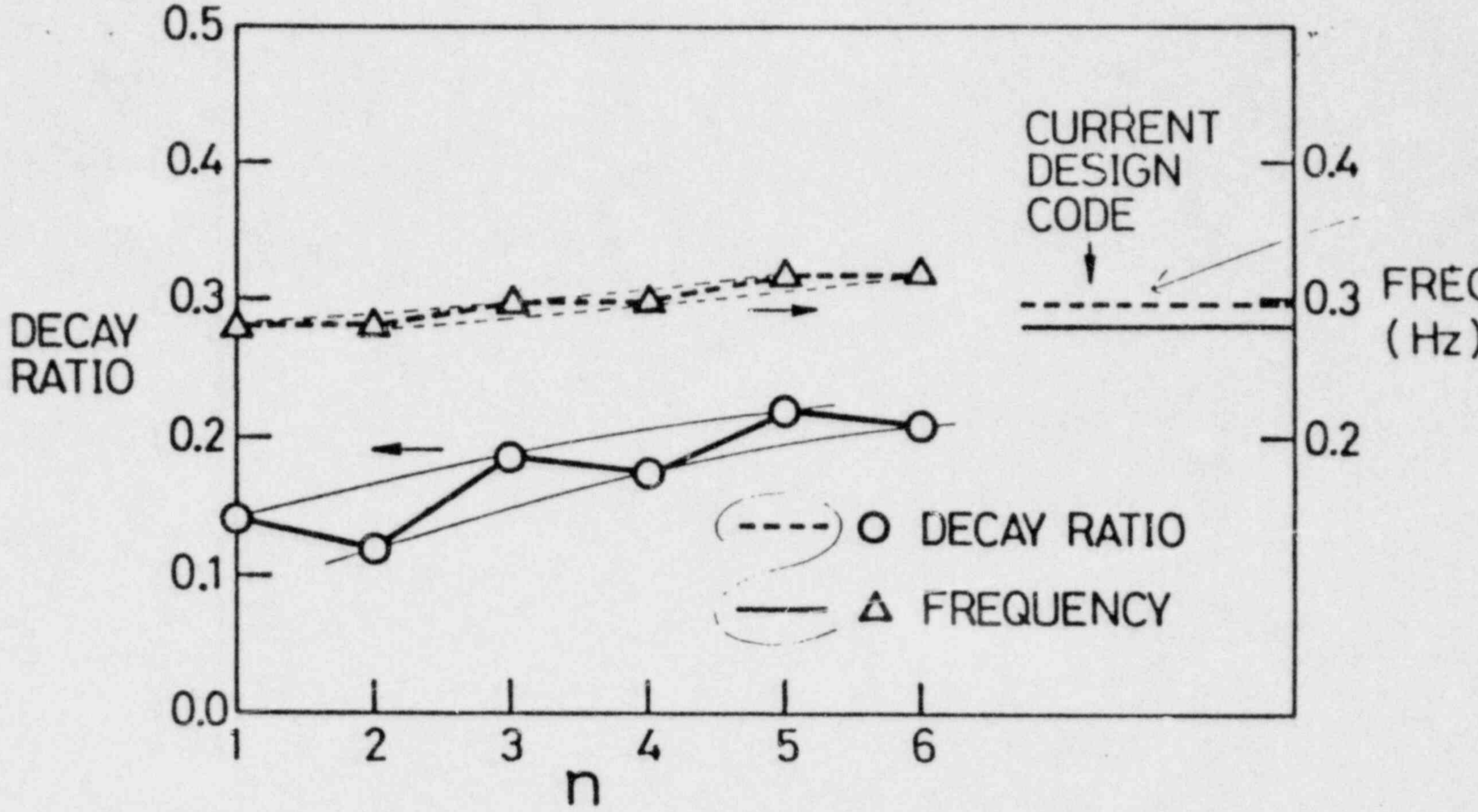

EFFECT OF PARALLEL CHANNEL

RESPONSE OF POWER TO RECIRCULATION HEAD 4 kPa STEP DOWN

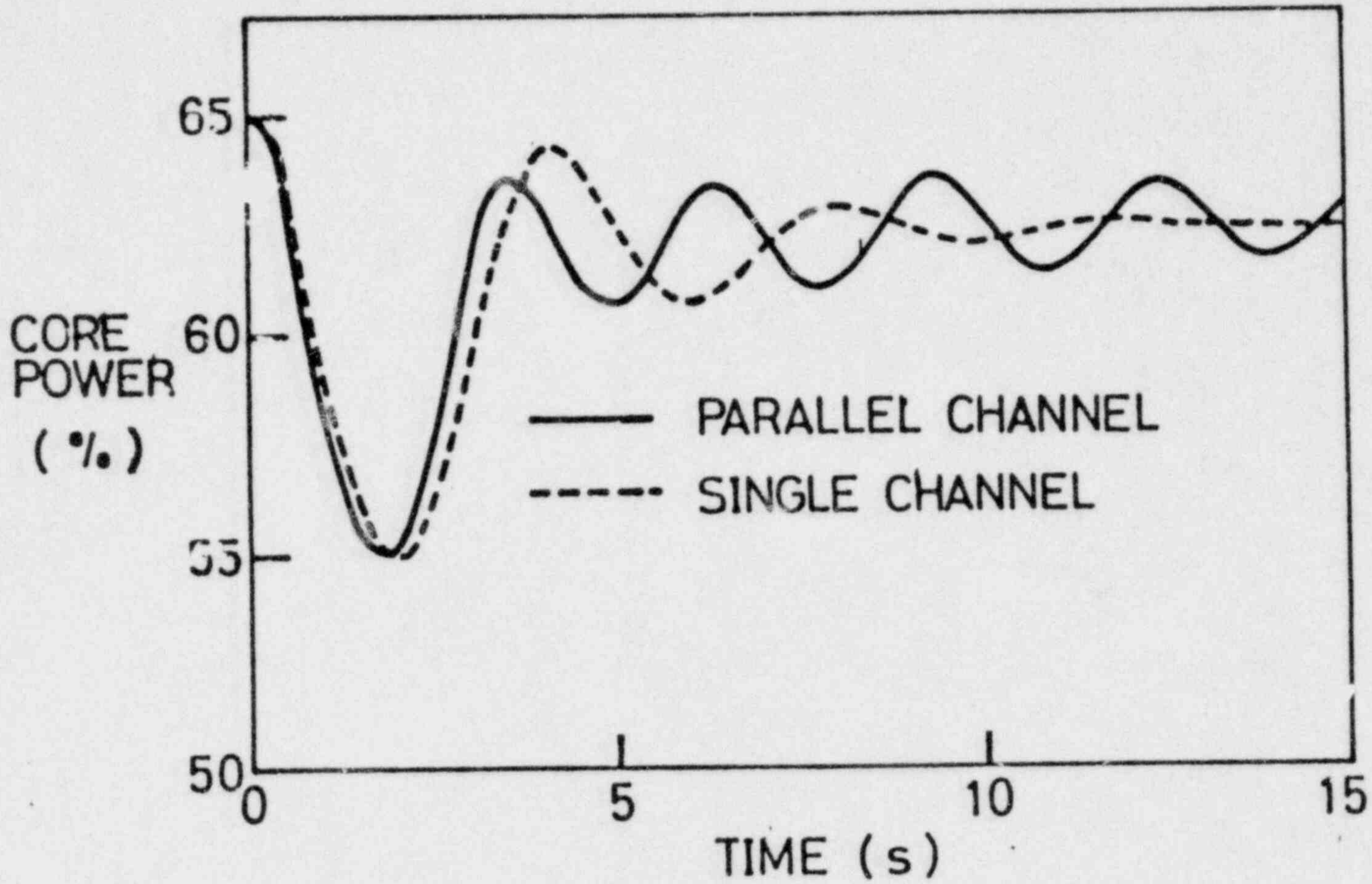

EFFECT OF PARALLEL CHANNEL

CHANNEL INLET FLOW CHANGE

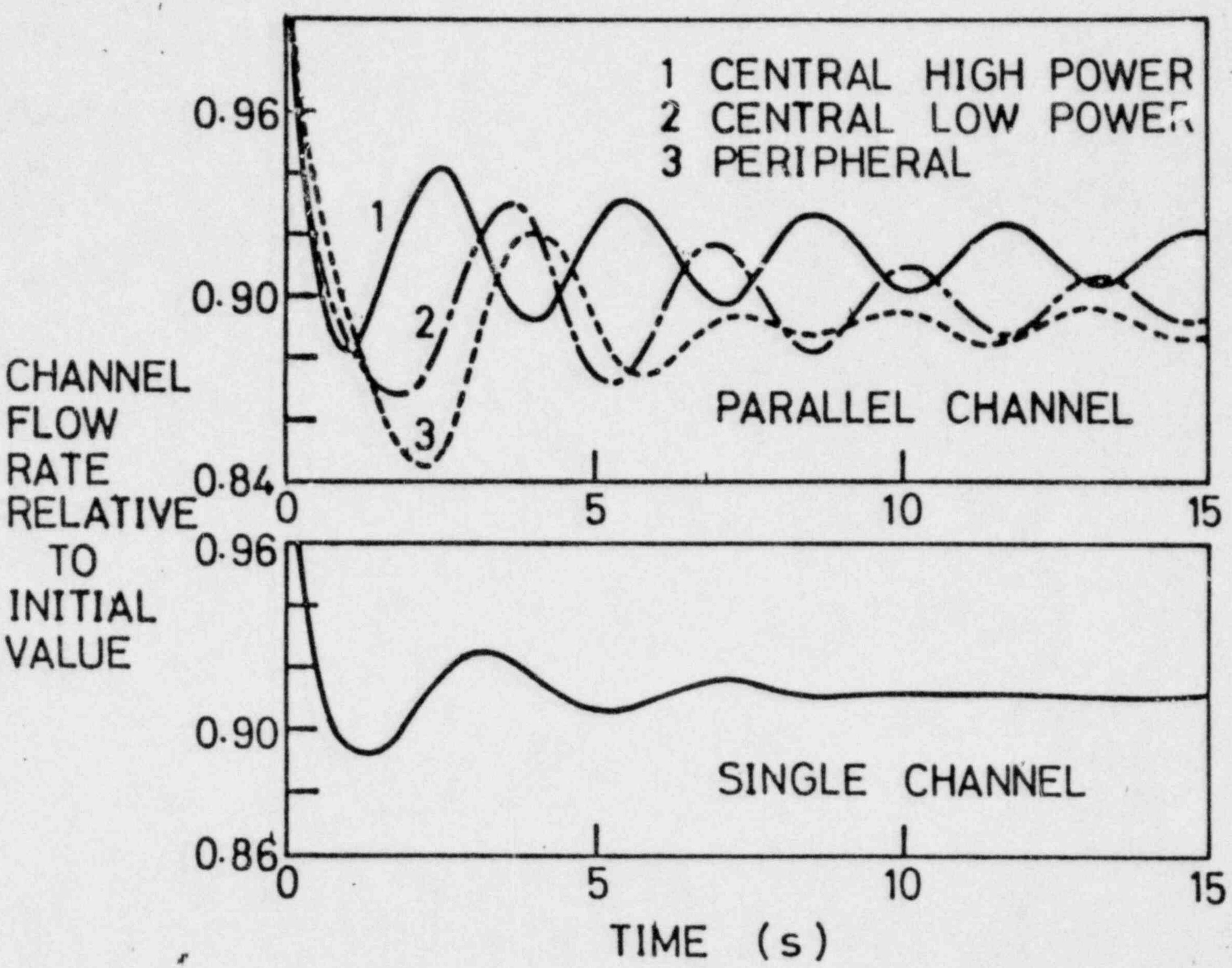

EFFECT OF PARALLEL CHANNEL

VOID FRACTION CHANGE AT MID-HEIGHT OF CORE

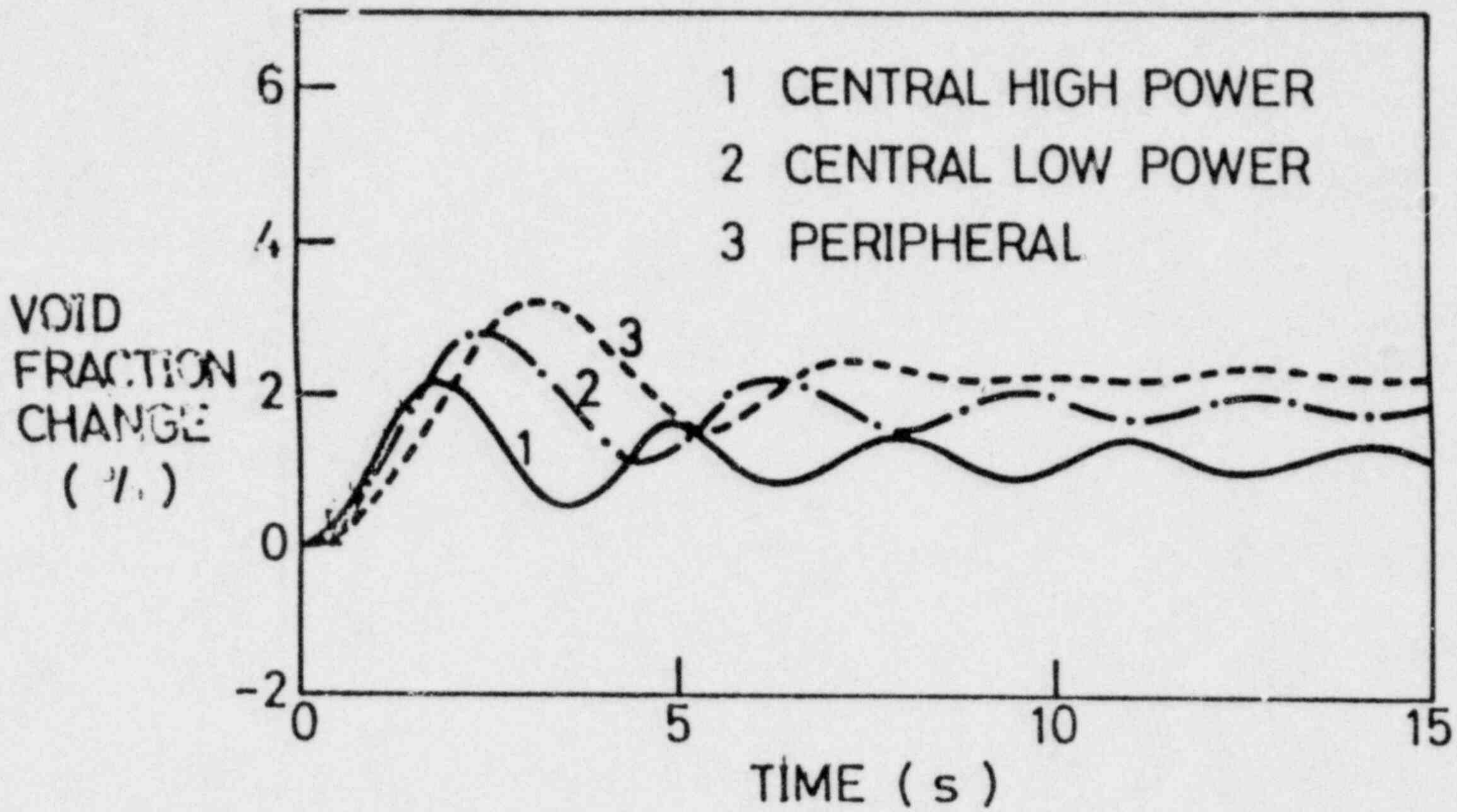

CONCLUSIONS

1. TIME DOMAIN STABILITY CODE DEVELOPED

   o PARALLEL CHANNEL CAPABILITY

   o POINT NEUTRON KINETICS

2. COMMERCIAL SIZE BWR ANALYZED

   o SMALLER DECAY RATIO THAN CURRENT DESIGN CODE

   o DECAY RATIO TEND TO INCREASE AS AMPLITUDE DECREASE
   (SEEM TO BE NONLINEARITY EFFECT)

   o PARALLEL CHANNEL EFFECT

      1) DESTABILIZE CORE

      2) OUT OF PHASE BEHAVIOR